



HAL
open science

A comprehensive study on the phenomenon of total breakthrough in liquid chromatography

Soraya Chapel, Florent Rouvière, Vincent Peppermans, Gert Desmet, Sabine Heinisch

► **To cite this version:**

Soraya Chapel, Florent Rouvière, Vincent Peppermans, Gert Desmet, Sabine Heinisch. A comprehensive study on the phenomenon of total breakthrough in liquid chromatography. *Journal of Chromatography A*, 2021, 1653, pp.462399. 10.1016/j.chroma.2021.462399 . hal-03324142

HAL Id: hal-03324142

<https://hal.science/hal-03324142>

Submitted on 2 Aug 2023

HAL is a multi-disciplinary open access archive for the deposit and dissemination of scientific research documents, whether they are published or not. The documents may come from teaching and research institutions in France or abroad, or from public or private research centers.

L'archive ouverte pluridisciplinaire **HAL**, est destinée au dépôt et à la diffusion de documents scientifiques de niveau recherche, publiés ou non, émanant des établissements d'enseignement et de recherche français ou étrangers, des laboratoires publics ou privés.



Distributed under a Creative Commons Attribution - NonCommercial 4.0 International License

1 **A comprehensive study on the phenomenon of total breakthrough in liquid chromatography**

2

3 Soraya CHAPEL^a, Florent Rouvière^a, Vincent Peppermans^b, Gert Desmet^b, Sabine Heinisch^{a*}

4

5 ^aUniversité de Lyon, Institut des Sciences Analytiques, UMR 5280, CNRS, 5 rue de la Doua, 69100,
6 Villeurbanne

7 ^bDepartment of Chemical Engineering, Vrije Universiteit Brussel, Pleinlaan 2, 1050 Brussel, Belgium

8 *Corresponding author:

9 Tel: +33 437 423 551

10 E-mail address: sabine.heinisch@univ-lyon1.fr

11

12

13 **Abstract**

14 Differences in elution strength between the sample solvent and the mobile phase usually give rise to
15 undesirable effects on the chromatographic separation, which may range from slight broadening to
16 severe peak deformation or even splitting. In the most extreme case, the retention factor of the
17 analyte at the head of the column is so small at the time of injection that part of the analyte goes
18 through the column with very little interaction with the stationary phase and hence elutes very close
19 to the column dead time. This phenomenon is known as breakthrough. Usually, during
20 breakthrough, the retained peak displays a wide array of deformations and it is not rare that
21 multiple retained peaks appear for a given injected analyte. However, under certain conditions, it
22 has been demonstrated that these deleterious effects could fully disappear, leaving only one
23 breakthrough peak and one symmetrical peak on the chromatogram. This so-called “total
24 breakthrough” phenomenon was recently highlighted in the specific context of the 2D-LC separation
25 of peptides but has yet to be explained. In the present paper, we describe the results of a
26 comprehensive study aiming to better understand and define the conditions of emergence of both
27 breakthrough and total breakthrough phenomena in liquid chromatography. The effects of a broad
28 range of parameters, including the nature of the solute, the retention mechanism, the injection and
29 elution conditions, the column temperature, and the injected sample concentration on the
30 occurrence of both phenomena were investigated. While breakthrough was found to occur for all
31 studied compounds, it appears that the presence of positive charges on the molecule is a
32 prerequisite for observing a total breakthrough phenomenon. Among all the parameters
33 investigated in this work, only the injection conditions and the analyte retention were found to be
34 impactful on the onset of both phenomena. This finding allowed us to suggest one necessary and
35 sufficient condition, relying on the injection of critical volumes to observe each respective

36 phenomenon. These critical volumes only depend on the column dead volume and the retention
37 factor of the analyte in the injection solvent.

38

39 **Keywords**

40 Total breakthrough phenomenon, liquid chromatography, injection solvent strength, peptides,
41 ionizable compounds

42

43

44 **1. Introduction**

45 In the quest for ever more sensitive, ever faster separations, and ever higher separation power,
46 comprehensive two-dimensional liquid chromatography (LC x LC) has acquired a place of choice
47 among separation methods [1–3]. One of the most limiting problems in LC x LC is related to injection
48 in the second dimension [4,5]. The injection solvent is often much stronger than the mobile phase
49 while the injection volume is usually much larger than the one in one-dimensional liquid
50 chromatography (1D-LC). This can result in very bad peak shapes including peak broadening, peak
51 distortion, and peak splitting, but also, in some cases, in the occurrence of a breakthrough
52 phenomenon. This phenomenon occurs for a given compound when the injected volume is so large
53 that part of the molecules elute with the solvent peak while the other part leaves the injection
54 solvent and leads to a retained peak with a long fronting tail. In addition to the retained peak, a
55 breakthrough peak is thus eluted close to the column dead time (sometimes just before, depending
56 on whether there is size exclusion or ionic repulsion).

57 The combination of hydrophilic interaction liquid chromatography (HILIC) with reversed-phase liquid
58 chromatography (RPLC) gives a typical example of this situation where the first dimension mobile
59 phase, and thus the injection solvent in the second dimension is very strong compared to the second
60 dimension mobile phase [6–13]. However, such a situation can also be encountered in 1D-LC, either
61 in RPLC with compounds poorly soluble in water-rich solvents or in HILIC with compounds poorly
62 soluble in acetonitrile-rich solvents. The phenomenon of breakthrough has been known for a long
63 time [14,15]. It was recently investigated in reversed phase liquid chromatography (RPLC) for neutral
64 species [16]. An excellent agreement was obtained between simulated and experimental
65 separations. In particular, the peak distortion which occupied the whole retention space between
66 the breakthrough peak and the retained peak could be well simulated [16]. It was also theoretically
67 demonstrated that breakthrough occurred above a critical injection volume, $V_{crit,B}$, which can be
68 related to the column dead volume, V_0 , by the following simple relationship:

$$69 \quad V_{crit,B} = k_s \times V_0 \quad (1)$$

70 Where k_s is the retention factor of the analyte in the injection solvent.

71 We recently pointed out a new phenomenon [7] which relies on the finding that, injecting a large
72 enough sample volume in RPLC resulted not only in a breakthrough peak but also yielded a
73 symmetrical retained peak (no peak distortion, no fronting tail). We called this phenomenon “total
74 breakthrough” in reference to the complete disappearance of the molecules between the
75 breakthrough peak and the retained peak above a critical injection volume, $V_{crit,TB}$, of course, larger
76 than $V_{crit,B}$. This phenomenon was shown to be highly repeatable. The retained peak areas were
77 found to vary linearly with the injected amount, provided that total breakthrough conditions were
78 established, which suggests that quantitative analysis is possible under these conditions. In a more
79 recent study, total breakthrough conditions were compared to more traditional approaches used in
80 HILIC x RPLC for maximizing peak capacity including post-¹D-flow splitting and on-line solvent
81 dilution. It was shown that total breakthrough conditions were the only approach that allowed to
82 have symmetrical peaks over the whole 2D-separation space [17].

83 In these two reported studies [7,17], the phenomenon of total breakthrough was presented as part
84 of the separation of peptides in RPLC at acidic pH. We have never encountered such a phenomenon
85 before, nor we are aware of any reports about it. In the present study, our objective was therefore
86 to know precisely which separation conditions in liquid chromatography and which compounds can
87 lead to this phenomenon. We were also interested in the critical volume ($V_{crit,TB}$) above which the
88 phenomenon of total breakthrough appears. Finally, we found it interesting to test and validate Eq.1
89 on experimental results.

90

91 **2. Experimental section**

92 **2.1. Chemicals**

93

94 Deionized water was produced using an Elga Purelab Classic UV purification system from Veolia
95 water STI (Décine-Charpieu, France). LC-MS grade acetonitrile (ACN), clozapine, protriptyline,
96 imipramine, amitriptyline, nadolol, propranolol, diphenhydramine, N,N-dimethylaniline, and salicylic
97 acid were purchased from Sigma-Aldrich (Steinheim, Germany). Analytical reagent grade ammonium
98 acetate (AA) and LC-MS grade formic acid (FA) were purchased from Fischer scientific (Illkirch,
99 France). Influenza hemagglutinin (HA), leucine enkephalin, bombesin, [arg8]-Vasopressin, [ile]-
100 angiotensin, bradykinin fragment 1–5, substance P, and bradykinin were obtained from Merck
101 (Molsheim, France). WDDHH was custom synthesized (Genecust, Luxembourg). The physical
102 properties of all the compounds studied are listed in Table 1.

103

2.2. Sample preparation

For small molecular weight (MW) compounds (MW < 350 Da), stock solutions of each analyte were prepared at a concentration of 200 mg/L in ACN/water (50:50 v/v) for clozapine, protriptyline, imipramine, amitriptyline, diphenhydramine, and salicylic acid or 1000 mg/L (0:100 v/v) for nadolol and N,N-dimethylaniline. For peptides, the stock solutions of each compound were prepared in pure water at 500 mg/L for influenza hemagglutinin, bombesin, [arg8]-vasopressin, [ile]-angiotensin, and substance P, 1000 mg/L for bradykinin, 1500 mg/L for WDDHH, 2500 for bradykinin fragment 1–5, and 5000 mg/L for leucine enkephalin. Most injected samples were prepared individually by appropriate dilution of each stock solution with water and acetonitrile. The final concentration was 50 mg/L for leucine encephalin and 0.5 mg/L for the small MW basic compounds unless stated otherwise. For Fig. S1, the injected samples were prepared by combining stock solutions of all small MW basic compounds (Fig. S1a) or all peptides (Fig. S1b) before adding an appropriate volume of acetonitrile. The final concentrations in these mixtures were 16 mg/L (peptides) and 1 mg/L (small MW basic compounds). The sample solvent composition of each prepared sample is indicated in the figure captions.

2.3. Instrumentation and columns

Chromatographic experiments were performed on two different systems. System 1 was used for the analysis of individually injected compounds, whereas System 2 was used for the injection of mixtures (Fig. S1) and the isocratic experiment. System 1 consisted of the first dimension of a 2D-LC ACQUITY UPLC I-Class instrument from Waters Corporation (Milford, MA, USA). It includes a binary solvent delivering pump (BSM), a sample manager with a flow-through needle (SM-FTN) injector equipped with a 15 μ L loop, a thermostated column manager, an ACQUITY photodiode-array detector (PDA) with a 0.5 μ L flow cell. For most experiments, an extension loop of 100 μ L was added to the injector. For the study of the effect of the isocratic hold at the beginning of the gradient, the experiments were performed without this extension loop. The measured dwell volume (V_D) and extra-column volume (V_{ext}) for this system were 110 μ L and 12 μ L, respectively (without extension loop). The LC system was hyphenated to an ACQUITY single quadrupole mass spectrometry detector (QDa). A zero dead volume T-piece was placed after the column to reduce the flow entering MS. The T-piece connected the column outlet to the QDa and PDA inlets via PEEK capillary tubings of 100 μ m inner diameter. It was designed to send half of the flow to UV and the other half to MS (split 1:1). Instrument control, data acquisition, and data handling were performed by MassLynx v4.1 software

138 (Waters Corporation). System 2 consisted of the first dimension of a 2D-LC 1290 Infinity II instrument
139 from Agilent Technologies (Waldbronn, Germany). It includes a binary pump (G7120A), and
140 autosampler (G7120B) with a flow-through needle injector equipped with a 20 μL loop, a
141 thermostated column compartment (G7116B), and a diode array detector (DAD) with a 0.6 μL flow
142 cell (G7117A). The measured dwell volume and extra-column volume for this system were 170 μL
143 and 22 μL , respectively. The system was hyphenated with a Q-TOF mass spectrometer (G6560B)
144 equipped with a 35 μL JetStream source (Agilent Technologies). The LC system was controlled by
145 OpenLAB CDS Chemstation Edition revision C.01.09 and the Q-TOF by MassHunter Acquisition
146 version B.09.00 software (Agilent Technologies). MS data handling was performed by MassHunter
147 Qualitative Analysis version B.10.0.10305.0 software.

148 An ACQUITY UPLC CSH C18 column (30 x 2.1 mm, 1.7 μm) was used in RPLC and an ACQUITY UPLC
149 BEH Amide column (50 x 2.1 mm, 1.7 μm) in HILIC. Both columns were obtained from Waters
150 Corporation. The measured column void volume (V_0) were 73 μL and 121 μL , respectively (total
151 porosity close to 0.7).

152

153 **2.4. Chromatographic and detection conditions**

154

155 For the RPLC experiments, unless otherwise stated, the column temperature was set at 80°C, the
156 flow rate was 1.5 mL/min, and gradient elution was used with 0.1% formic acid in water as solvent A
157 (pH 2.7) and 0.1% formic acid in ACN as solvent B. The solvent gradient was: 1-45-1-1% B in 0-0.54-
158 0.59-1 min (corresponding to a normalized gradient slope of about 4%). As part of this study, the
159 following elution conditions were varied to assess their impact on the separations: the composition
160 of ACN at initial conditions (1, 5 or 10% B), the normalized gradient slope (1, 4, 8 or 12%), the
161 duration of the isocratic hold at the beginning of the gradient (0, 0.13, 0.27 or 0.53 min), the flow
162 rate (0.75 or 1.5 mL/min), and the temperature (30 or 80°C). These specific elution conditions are
163 indicated in the figure captions. Depending on the conditions, the injected volumes varied from 0.35
164 μL to 72 μL (corresponding to about 0.5% V_0 to 99% V_0).

165 In isocratic elution, the flow rate was 0.5 mL/min and the mobile phase composition was 0.1%
166 formic acid in water/0.1% formic acid in ACN 90:10 (v/v).

167 At neutral pH, the column temperature was 30°C, the flow rate was 0.75 mL/min, the mobile phase
168 consisted of 10 mM ammonium acetate in water as solvent A (pH 6.8) and ACN as solvent B, and the
169 solvent gradient was: 1-55-1-1% B in 0-1.33-1.43-3 min.

170 In HILIC, the column temperature was 30°C, the flow rate was 0.6 mL/min, and the mobile phase
 171 consisted of ACN as solvent A and 10 mM ammonium acetate in water as solvent B (pH 6.8). The
 172 solvent gradient was 2-60-2-2% B in 0-5.8-6-8 min.

173 UV chromatograms were recorded at 210 nm with an acquisition rate of 40 Hz. The QDa ionization
 174 source was used in the ESI positive mode for most compounds and negative mode for salicylic acid
 175 with Selected Ion Recording (SIR). Data were acquired between 100 and 350 Da for small MW
 176 compounds, and 500 and 1250 Da for peptides, with an acquisition rate of 10 Hz. Nitrogen (N₂) was
 177 used as a drying gas. The source temperature was maintained at 125°C. The capillary voltage was set
 178 at 0.8 kV, the probe temperature at 600°C, and the cone voltage at 15 V.

179 QTOF-HRMS data were acquired in ESI positive mode between 100 and 1700 Da with an acquisition
 180 rate of 20 spectra/s. The drying gas temperature and flow rate were set at 200°C and 11 L/min,
 181 respectively. The nebulizer gas pressure was set at 40 psi. The sheath gas temperature and flow rate
 182 were set at 350°C and 11 L/min, respectively. The capillary, the nozzle, the fragmentor, the skimmer,
 183 and the Oct 1 RV voltages were set at 3500, 300, 150, 20, and 750 V, respectively.

184

185 2.5. Calculations

186 The gradient profile at the column outlet is shown in the different figures (dotted lines with Y-scale
 187 on the right). It is related to the composition of the mobile phase at analyte elution, calculated
 188 according to the following relationship:

$$189 C_{elution} = C_{initial} + \frac{(C_{final} - C_{initial})}{t_G} (t_r - t_D - t_0) \quad (2)$$

190 Where $C_{initial}$ and C_{final} are the initial and final compositions of eluting solvent in the mobile phase, t_r
 191 is the retention time, t_D is the total dwell time, and t_0 is the column dead time.

192

193 The normalized gradient slope is the product of the gradient slope and the column dead time:

$$194 s = \frac{\Delta C}{t_G} \times t_0 \quad (3)$$

195 Where ΔC and t_G are the gradient composition range and the gradient time, respectively.

196

197 The intercept, $\log(kw)$, and the slope, S_{log} , of the relationship between the logarithm of the retention
 198 factor and the volume fraction of the strong solvent were calculated from two gradient runs using
 199 OSIRIS software (V 4.2, Euradif, Grenoble, France) with an Acquity CSH C18 (150 x 2.1 mm, 1.7 μ m)
 200 column at 80°C (A: water + 0.1% FA, B: ACN + 0.1% FA; 1% B to 41% B in 10 min and 30 min;
 201 0.7mL/min). The values are given in Table 1.

202

203

204 3. Results and discussion

205

206 3.1. Determination of the compounds involved by total breakthrough

207

208 As stated above, total breakthrough (TB) has been defined in circumstances where there are two
209 distinct peaks for a given solute, the first one non-retained (breakthrough peak) and the second one,
210 retained and quite symmetrical [7]. Thus, the conditions required, for a given compound, to
211 recognize a total breakthrough situation are: (i) the presence of a breakthrough peak, (ii) the
212 presence of a retained peak, which should be quite symmetrical, (iii) the absence of compound
213 molecules detected between the breakthrough peak and the retained peak (i.e. no middle peak and
214 no peak fronting should be observed).

215 It was found for peptides that TB occurred when the injection volume was higher than a critical one.
216 For smaller volumes, between the critical breakthrough volume ($V_{crit,B}$) and the critical TB volume
217 ($V_{crit,TB}$), a transition step was pointed out, in which breakthrough occurred while the retained peak
218 was distorted and sometimes split. It should be noted that we were not interested in this study by a
219 possible deformation of the breakthrough peak but by the deformation of the retained peaks and
220 furthermore by the absence of deformation of the retained peaks beyond a given injection volume,
221 which is a completely counterintuitive situation that has never been reported before. In this section,
222 the phenomenon of breakthrough is studied for different solutes (neutral, acid, basic, peptides) in
223 different chromatographic conditions including RPLC at acidic pH, RPLC at neutral pH, and HILIC, with
224 the objective of identifying the conditions required for the emergence of total breakthrough.

225

226 3.1.1. In RPLC at acidic pH

227 The occurrence of breakthrough and sometimes total breakthrough in RPLC at acidic pH is
228 highlighted in Fig.1. Various volumes were injected for four different compounds. These include
229 caffeine (neutral at this pH), leucine enkephalin (multi-charged compound with $pI = 6.0$), propranolol
230 (weak base with $pK_a = 9.4$), and salicylic acid (weak acid with $pK_a = 3.0$). Their separations were
231 obtained in RPLC under acidic conditions (pH 2.8). The injection solvent strength was rather high
232 (50:50 water/ACN), thus leading to a significant difference between the injection solvent and the
233 composition of the mobile phase at peak elution (of the order of 35% ACN). In these acidic
234 conditions, both leucine enkephalin and propranolol were expected to be mainly positively charged,
235 whereas salicylic acid was expected to be mainly in its acid form (uncharged). The same gradient
236 conditions were applied to all solutes. The ratio of the injection volume to the column dead volume
237 (V_i/V_0) was increased (from the top of Fig. 1 to the bottom) in order to study its impact on the

238 separation. The dotted lines represent the evolution of the composition at elution with the analysis
239 time

240 As can be observed, when the injection volume is low enough (i.e. $V_i/V_0 = 1\%$ here), there is only one
241 retained peak, nearly symmetrical whatever the solute. As the injected volume increases (2nd row of
242 chromatograms), the peaks of caffeine (Fig.1a) and salicylic acid (Fig.1d) are broadened and even
243 distorted, while those of leucine enkephalin (Fig.1b) and propranolol (Fig.1c) are split, resulting in
244 the latter case in the appearance of a second peak with smaller retention.

245 For large enough injection volumes, a breakthrough peak (marked with an asterisk) appears for all
246 solutes. As can be observed in Fig.1, $V_{crit,B}$ was between 5% and 10% V_0 for caffeine, 3% and 4.8% V_0
247 for both leucine enkephalin and propranolol, and larger than 50% V_0 for salicylic acid. In the case of
248 caffeine and salicylic acid, the breakthrough peak and the retained peak are always connected by a
249 bridge of molecules, even well beyond $V_{crit,B}$. Furthermore, from the moment the retained peak
250 starts to broaden, peak distortion consistently increases as the injection volume increases. Unlike
251 these two compounds for which TB could therefore not be attained whatever the volume injected
252 (up to 140% V_0 in this study), TB can be observed for both leucine enkephalin and propranolol
253 (bottom chromatogram in Fig. 1b and Fig. 1c, respectively). For both compounds, $V_{crit,TB}$ was between
254 4.8% and 6.2% V_0 , hence slightly larger than $V_{crit,B}$. It is important to note that, between $V_{crit,B}$ and
255 $V_{crit,TB}$, three distinct peaks are present on the chromatogram. In the rest of this study, we will refer
256 to each of these three peaks as “breakthrough peak”, “middle peak” and “retained peak”,
257 respectively.

258 The fact that the trend for leucine enkephalin and propranolol was exactly the same can be related
259 to the similarity of their retention model coefficients (k_w and S_{log} given in Table 1), thereby leading
260 to very close retention times. Since the main difference between these two compounds is their size,
261 this suggests that this phenomenon is independent of diffusion. Similar results were obtained with
262 different peptides and different weak bases exhibiting various retention times (various coefficients
263 as shown in Table 1) under the same chromatographic conditions. The resulting separations of these
264 compounds are shown in Fig. S1. In all cases, the retained peak was narrow and rather symmetrical
265 as long as the injected volume was above a specific $V_{crit,TB}$ value. It should be pointed out that similar
266 results were also obtained on a BEH C18 column, as highlighted in Fig. S2.

267 From these preliminary results, two important conclusions can be drawn: (i) under acidic conditions,
268 while breakthrough can be achieved with any compound as long as it exceeds the critical volume
269 ($V_{crit,B}$), total breakthrough appears to be achievable only with positively charged compounds such as
270 peptides or weak bases, (ii) the advantages of TB conditions, in terms of peak shape, previously
271 highlighted for peptides [7] should apply to weak bases as well.

272 All the above-discussed results were obtained in gradient elution. It is interesting to note that the
273 trend was somewhat different in isocratic elution. As exemplified for leucine enkephalin in RPLC at
274 acidic pH (Fig. 2), the shape of the retained peak at an early stage of breakthrough ($V_i/V_0 = 3.4\%$)
275 seems to be similar to the one obtained with neutral compounds in gradient elution (Figs. 1a and
276 1d), with a continuous bridge of molecules between the breakthrough and the retained peaks.
277 However, unlike neutral compounds, the bridge height decreases almost down to the baseline above
278 a critical injection volume ($V_{crit,TB}$ value of about $6.9\% V_0$) which reminds a total breakthrough
279 situation. However, unlike gradient elution, the retained peak is not quite symmetrical but exhibits
280 low fronting regardless of the injection volume above $V_{crit,TB}$.

281

282 3.1.2. In RPLC at neutral pH

283 The first question that naturally arises from the preceding results is whether or not the charge of the
284 molecule plays a part in the occurrence of total breakthrough. To answer this question, we
285 performed the same study as in Fig. 1, but under neutral conditions (pH 6.8). Propranolol (very
286 strongly retained in such conditions) was replaced by N,N-dimethylaniline (pKa of 5.1). The main
287 stages of the separation according to the injection volume, are shown in Fig. 3 for the peptide (Fig.
288 3a), the weak base (Fig.3b), and the weak acid (Fig. 3c). The sample solvent consisted of a mixture of
289 water/ACN (30:70 or 50:50, v/v). Under these pH conditions, N,N-dimethylaniline was expected to
290 be mainly neutral, salicylic acid to be negatively charged, while the dominant form of leucine should
291 be the zwitterion (N-terminus protonated, uncharged chain, and C-terminus deprotonated). As
292 shown in Fig. 3a, the trend for leucine enkephalin at neutral pH is quite the same as at acidic pH (see
293 Fig. 1b) despite the presence of as many negative charge as positive charge on the molecule. By
294 increasing the injected volume, the separation goes through a single symmetrical peak ($1\% V_0$) to the
295 occurrence of breakthrough ($4.8\% V_0$) and then total breakthrough ($9.6\% V_0$). A middle peak with
296 intermediate retention is observed, without ($3.9\% V_0$) or with ($4.8\% V_0$) breakthrough. The same
297 trend was also observed for more acidic peptides (lower pI) as well as for more basic peptides
298 (higher pI) as exemplified in Fig. S3 for influenza hemagglutinin and bradykinin fragment 1-5,
299 respectively. For N,N,dimethylaniline (Fig. 3b), the trend at neutral pH is similar to the one observed
300 for any neutral compound regardless of pH [16]. $V_{crit,B}$ is high and close to $77\% V_0$. By further
301 increasing the injected volume, the retained peak exhibits an increasing fronting, which persists
302 even with very large injected volumes ($> 99\% V_0$). For salicylic acid (Fig. 3c), the trend is different.
303 The retained peak exhibits a fronting shoulder with injection volumes as low as $2.8\% V_0$. By
304 increasing the injection volume, a middle peak appears ($3.4\% V_0$) and then a breakthrough peak
305 ($V_{crit,B}$ between $3.4\% V_0$ and $4.8\% V_0$). However, unlike positively charged compounds, a complete

306 baseline resolution was never achieved between the breakthrough peak and the retained peak. Both
307 remained connected by a continuous bridge of molecules, the height of which increased with the
308 injected volume. In other words, total breakthrough was never observed for this negatively charged
309 analyte.

310 To summarize, we only observed a total breakthrough phenomenon with positively charged
311 compounds (here peptides and small pharmaceuticals). With neutral or anionic compounds, the
312 shape of the retained peak got worse and worse as the injection volume increased. These results
313 suggest that only the presence of positive charges on the molecule leads to the occurrence of total
314 breakthrough. In this specific case, an unexplained phenomenon appears during the injection
315 process, which divides the molecules into different populations (two or three depending on whether
316 there is a middle peak or not) that will travel through the column at different linear velocities during
317 the separation process. The resulting separation and the resulting peak shapes cannot be accurately
318 predicted with the previously developed approach [16] which has been shown to work well with
319 neutral compounds. The different behaviour between neutral/negatively charged and positively
320 charged analytes is certainly difficult to explain. The first explanation that comes to mind is that this
321 phenomenon is related to the mixed retention mechanism (on both alkyl chains and ionized silanols)
322 that exists in RPLC with protonated compounds on silica-based columns. These two mechanisms
323 have different kinetic interactions (fast for hydrophobic interaction while slow for electrostatic
324 interaction) [18], which might support the existence of different populations. However, solute
325 retention is a thermodynamic process that makes the solutes continuously adsorbing and desorbing
326 during their travel through the column. Furthermore, against an explanation based on a mixed
327 retention mechanism, total breakthrough was observed for positively charged compounds at low pH
328 (i.e. 2.7) where there are very few ionized silanols. We are, therefore, still working on finding a
329 possible explanation.

330 **3.1.3. In HILIC**

331 The phenomenon of total breakthrough was also observed for peptides in HILIC. An example is given
332 in Fig. 4, showing the evolution of elution profiles of leucine enkephalin with the injected volume
333 after dissolution in a strong solvent (i.e. pure water). Below 10% V_0 injected, the peaks were split
334 into two (1% V_0) or multiple distinct peaks (2% V_0), until the occurrence of breakthrough with the
335 presence of a broad middle peak (5% V_0). Interestingly, the presence of multiple distinct peaks
336 before the emergence of breakthrough was never observed in RPLC. Above 10% V_0 injected, the
337 middle peak completely disappeared, leaving only two peaks on the chromatogram, the
338 breakthrough peak and a narrow and symmetrical retained peak. Those results were obtained on a
339 BEH amide column but similar observations were made using a BEH HILIC column (bare silica), as

340 shown in Fig. S4. The retention mechanism in HILIC is known to be multimodal [19,20]. For ionized
341 compounds such as peptides, it might involve partitioning between the organic-rich mobile phase
342 and the water-enriched layer partially immobilized on the stationary phase, electrostatic interaction
343 (attractive or repulsive) between the charged analyte and the residual silanols, and hydrogen
344 bonding with the stationary phase. From our perspective, the fact that the peptide behaviour seems
345 to be similar in HILIC and RPLC might also be related to the existence of secondary interactions.
346 However, as in RPLC, it is quite difficult to explain the reasons for which distinct peaks are present,
347 and above all, why total breakthrough emerged with positively charged compounds only.

348

349 **3.2. Identification of the relevant factors affecting breakthrough and total breakthrough**

350

351 In this part of the work, we evaluated the effect of various parameters on the emergence of
352 breakthrough and total breakthrough. The study was carried out in RPLC with positively charged
353 analytes eluted in gradient elution at acidic pH. The investigated parameters included the eluent
354 strength of the injection solvent, the gradient conditions, the column temperature, and the
355 concentration of the analyte. The goal of this study was to make progress in the understanding of
356 the phenomenon of total breakthrough.

357

358 **3.2.1. Effect of the injection solvent composition**

359 Fig. 5 illustrates the effect of the injection solvent composition on the elution profiles of leucine
360 enkephalin. Figs. 5a to 5d show the results obtained with an organic solvent content ranging from
361 30% ACN to 90% ACN in the injection solvent, respectively. In each figure, a given colour is related to
362 a given peak shape in order to highlight the similarities between the four injection solvents. For
363 example, the red curves reflect conditions for which a single symmetrical peak is observed on the
364 chromatogram, whereas the purple curves capture the onset of total breakthrough. The first
365 observation that can be made when comparing Figs. 5a-d is that the evolution of the elution profile
366 with the injection volume is the same regardless of the eluent strength of the injection solvent. For
367 the four conditions of injection solvent depicted in Fig.5, the separation goes through the same
368 stages: (i) no injection issues (red curve), (ii) peak broadening (orange curve), (iii) appearance of a
369 middle peak (green curve), (iv) emergence of breakthrough with persistence of this middle peak
370 (blue curve), and (v) occurrence of total breakthrough (purple curve). The only difference is that
371 injection issues start with smaller injection volumes when the injection solvent is stronger (i.e. with a
372 larger content of acetonitrile). Whereas $V_{crit,TB}$ represents about 13.8% V_0 with 30% ACN in the
373 sample solvent (Fig. 5a), it is close to 3.4% V_0 with 90% ACN (Fig. 5d). Similar observations can be

374 made for the emergence of breakthrough, which appears with injection volumes of about 9.6% and
375 2.5% V_0 with 30% ACN (Fig. 5a) and 90% ACN (Fig. 5d), respectively. It is interesting to point out that
376 $V_{crit,TB}$ seems to be slightly higher than $V_{crit,B}$ (about 40 % higher) regardless of the injection solvent
377 composition (i.e. $V_{crit,TB} = 1.4 V_{crit,B}$). Considering Eq. 1, this means that the following relationship
378 could be used to estimate $V_{crit,TB}$ in the current conditions of the study:

$$379 \quad V_{crit,TB} = 1.4 \times k_s \times V_0 \quad (4)$$

380 In the case of leucine enkephalin, this implied that very small differences in injection volume (e.g. <
381 0.7 μ L in Fig. 5d) were sufficient to go from one phenomenon (i.e. breakthrough) to the other (i.e.
382 total breakthrough). It is important to note that it was not our purpose to accurately measure V_0 and
383 k_s but to establish a simple relationship relating these two parameters to $V_{crit,TB}$ as can be done with
384 $V_{crit,B}$.

385 The comparison of both the width and the shape of the retained peak, once the middle peak has
386 appeared (blue curve), is interesting. With 30% ACN (Fig. 5a), the peak is larger than with 90% ACN
387 (Fig. 5d) and furthermore exhibits a slight fronting. This trend is maintained under total
388 breakthrough conditions (purple and black curves). The fact that better retained-peak shapes were
389 obtained with stronger sample solvents is counter-intuitive. Furthermore, with the same injected
390 volume of 50 % V_0 (black curves in Fig.5), both the width and the shape of the retained peak are
391 clearly improved when the percentage of acetonitrile in the injection solvent increases.
392 Nevertheless, black and purple curves show that rather good peak shapes were obtained with very
393 large injection volumes once total breakthrough conditions have been attained. Another effect
394 occurring for very large injected volumes was the broadening and, in some cases, the splitting of the
395 breakthrough peak. As expected, for a given injection volume (e.g. 50% V_0), its shape is more
396 affected by stronger sample solvents. On the other hand, with stronger injection solvents, the shape
397 of the retained peak improves but its area decreases. For example, with 50% V_0 (black curve), the
398 retained peak area was about three times larger with 30% ACN (Fig. 5a) than with 90% ACN (Fig. 5d).
399 This is in agreement with the fact that a larger number of molecules are retained when the injection
400 solvent is weaker.

401 An interesting point to discuss is the evolution of the separation of the middle peak with the
402 injection volume, which is exemplified in Fig. S5 with 70% ACN as injection solvent. The trend was
403 found to be the same regardless of the injection solvent. In Fig. S5, the asterisk and the diamond
404 indicate the breakthrough and the retained peaks, respectively. The middle peak is located between
405 them. As seen, both its retention and its height progressively decreases with the injection volume.
406 The peak height is maximum when the middle peak is fully resolved from the retained peak (purple
407 curve). Then, it progressively decreases as the injection volume increases, while the peak width

408 increases. Once breakthrough has emerged (yellow curve), the retention and the width are no
409 longer evolving. At this point, the beginning of the middle peak is close to the onset of the gradient
410 (about 0.2 min). As the injection volume further increases, the peak height of the middle peak
411 decreases until the peak completely disappears when total breakthrough occurs (red curve). During
412 all these stages, the height and the area of the retained peak (diamond) remained approximately the
413 same. As highlighted in our previous work [7] and shown in Fig. 5 (purple curve vs. black curve), both
414 the height and the area of the retained peak start to increase again with the injected volume once
415 total breakthrough has emerged. The appearance and the evolution of this middle peak are very
416 surprising and totally unexplained so far. The understanding of the different separation stages
417 preceding total breakthrough will be necessary to be able to predict and simulate the separations
418 under total breakthrough conditions.

419

420 **3.2.2. Effect of gradient conditions**

421

422 **○ Initial mobile phase composition**

423

424 Fig. 6 shows the effect of the initial composition of the mobile phase on the peak profile of leucine
425 enkephalin. Three initial percentages of acetonitrile (strong solvent B) were studied: 1% (Fig. 6a), 5%
426 (Fig. 6b), and 10% (Fig. 6c). The gradient elution was carried out from the indicated initial
427 composition to the same final composition of 45% B while keeping the normalized gradient slope
428 constant by adjusting the gradient time. Consequently, the compositions at elution were similar. The
429 same volume ($2.5\% V_0$) was injected in the same solvent (50% ACN). As observed in Fig.6, injection
430 issues are more critical when the initial percentage of acetonitrile is higher. With 1% ACN (Fig. 6a),
431 the retained peak is split with no breakthrough. With 5% ACN (Fig. 6b), the middle peak is fully
432 resolved from the retained peak and still no breakthrough has appeared. With 10% ACN (Fig. 6c),
433 total breakthrough can be observed. This progression is comparable to what was observed when
434 increasing the injected volume for a given injection solvent strength (Fig. S5) or the injection solvent
435 strength for a given injected volume (Fig. 5). Our hypothesis to explain this effect is that the injection
436 plug is partly diluted in the initial mobile phase before entering the column, making the actual
437 injection solvent weaker (i.e. k_s higher) with 1% ACN as initial composition than with 10% ACN.

438

439 **○ Gradient time**

440 Fig. 7 shows the effect of the gradient time on the separation of leucine enkephalin. The separations
441 were obtained with four different gradient times corresponding to $44t_0$ (Fig. 7a), $11t_0$ (Fig. 7b), $5.5t_0$

442 (Fig. 7c), and $3.7t_0$ (Fig. 7d), thus leading to four different normalized gradient slopes (i.e. 1%, 4%,
443 8%, and 12%, respectively). The four injection volumes show all the stages of the separation, i.e.,
444 from a single symmetrical retained peak (black curve) to total breakthrough (orange curve). The first
445 observation that can be made is that, for a given injection volume (given colour in Fig. 7), the
446 separations appear very similar, suggesting that the gradient time does not play a part in the onset
447 of the different separation stages and, in particular, in the emergence of total breakthrough. The
448 same set of separation stages is observed regardless of the gradient time: (i) one peak without
449 breakthrough (black curve, 1% V_0), (ii) two peaks without breakthrough (purple curve, 3.0% V_0), (ii)
450 three peaks including the breakthrough peak (blue curve, 4.8% V_0), and (iv) total breakthrough
451 (orange curve, 6.9% V_0). For a given separation stage, the resolution between the middle and
452 retained peaks decreases with the gradient time, which can be related to the decrease in peak
453 capacity. Similar observations were made for two other peptides (bombesin and [ile]-angiotensin)
454 and two small pharmaceuticals (nadolol and propranolol) (data not shown). The fact that both
455 breakthrough and total breakthrough appear with the same injected volume regardless of the
456 gradient time is in good agreement with the fact that both $V_{crit,B}$ and $V_{crit,TB}$ are only dependent on k_s ,
457 and hence totally independent of the gradient time.

458

459

- **Initial isocratic hold duration**

460

461 The same observations were made when changing the isocratic hold duration as shown in Fig. 8 for
462 two compounds ([ile]-angiotensin and nadolol) with similar retention but markedly different
463 molecular weights (see Table 1). Both the gradient time (i.e. 1.08 min) and initial composition (i.e.
464 1%) were unchanged while the initial hold duration was varied from 0 min (Fig. 8a) to 0.53 min (Fig.
465 8c), leading to a total delay time (including the instrument dwell time) between 0.15 min and 0.68
466 min. The overlaid separations correspond to three injection volumes (1%, 1.2%, and 1.5% V_0). The
467 two analytes were weakly retained in such conditions and eluted at the very beginning of the
468 gradient elution (composition at elution close to 5% ACN) as shown by the gradient profile (dotted
469 lines). This explains why injection issues could already be observed with very small injected volumes
470 (<1% V_0) and why very small variations (i.e. $\pm 0.2\%$ V_0) significantly modified the separations. For
471 both analytes, injecting 1.0% V_0 (black curves) resulted in the appearance of two peaks without
472 breakthrough, whereas 1.2% V_0 (purple curves), and 1.5% V_0 (blue curves) were sufficient to trigger
473 breakthrough and total breakthrough, respectively. Similar to the effect of the gradient time,
474 different observations are noteworthy in Fig. 8: (i) the different stages of the separation and in
475 particular $V_{crit,B}$ (close to 1.2% V_0) and $V_{crit,TB}$ (close to 1.5% V_0) are quite the same regardless of the

476 duration of the isocratic hold and the analyte, (ii) the ratio between those values are once again
477 close to 1.4 (to the nearest measurement of uncertainty), (iii) the only difference in behaviour
478 between the two analytes is the width and the shape of the middle peak of nadolol which is broader
479 and less retained than that of [ile]-angiotensin, and (iv) the initial hold does not seem to affect the
480 different stages of the separation but it does impact the shape and the position of the middle peak.
481 In the case of [ile]-angiotensin, with 1.2% V_0 injected (purple curves in Figs. 8c), the middle peak
482 flattens out so much that it seems to completely disappear. However, as shown by the zoomed
483 figures (Fig. S6a), it is still present, suggesting that the situation of total breakthrough has not yet
484 been achieved.

485

486 ○ **Flow rate**

487

488 The effect of the flow rate is shown in Fig. 9 for [ile]-angiotensin (Figs. 9a/b on the left) and nadolol
489 (Figs. 9c/d on the right). The study was performed at 1.5 mL/min (Figs. 9a/c on the top) and 0.75
490 mL/min (Figs. 9b/d on the bottom). The normalized gradient slope was kept constant (i.e. $s=4\%$) by
491 changing the gradient time. As previously observed, for both compounds, there is no major
492 difference in the separation between the two flow rates except a less good separation at 1.5 mL/min
493 between the retained and the middle peak of [ile]-angiotensin which seems to result in a slightly
494 larger injection volume for the emergence of total breakthrough ($>1.2\% V_0$ at 1.5 mL/min vs $< 1.2\%$
495 V_0 at 0.75 mL/min). For nadolol, the trend at both flow rates is exactly the same. As shown in Fig. S7,
496 the same conclusions could be drawn for amitriptyline, a more retained base ($C_e = 23\%$ ACN), for
497 which the similarity of the separations between the two flow rates is remarkable.

498 As also previously underlined, the middle peak is larger and more distorted for nadolol than for the
499 peptide. Also, for nadolol, the retention shift of the middle peak is progressive when increasing the
500 injected volume until co-elution with the breakthrough peak. That was not the case for peptides,
501 [ile]-angiotensin (Figs. 9a/d) or leucine enkephalin (Fig. S5) although a similar trend was sometimes
502 noticed for little retained peptides as exemplified in Fig. S8. It is interesting to note that, since
503 nadolol and [ile]-angiotensin have a similar retention model (see Table 1), a possible relevant
504 difference between them is their molecular weight, which might suggest an effect of molecular
505 diffusion on the middle peak behaviour.

506

507 **3.2.3. Effect of the column temperature**

508

509 To highlight a possible effect of molecular diffusion, the column temperature was decreased from
510 80°C to 30°C, with a flow rate of 0.75mL/min. The obtained separations at 30°C for [ile]-angiotensin
511 (Fig.10a) and nadolol (Fig.10b) can be compared to those at 80°C shown in Figs. 9c and 9d,
512 respectively. In addition to a decrease in the solute diffusion coefficients, a reduction of
513 temperature can have other effects: (i) a variation of both mobile phase pH and solute pK_as
514 and hence a change in the solute ionization; (ii) a variation of the thermodynamic
515 equilibrium, thereby increasing distribution constants and hence the retention factors,
516 including k_s . As can be observed, the separations evolve in a similar way at the two studied
517 temperatures. As shown in Fig. S9, similar conclusions could be drawn for amitriptyline (more
518 retained basic compound). Yet, it is interesting to point out the significant difference in both the
519 shape and the retention of the middle peak for nadolol between 30°C (Figs. 10b) and 80°C (Fig. 9d).
520 The middle peak is indeed thinner and more retained at 30°C, resulting in a similar behaviour to the
521 peptide, unlike at 80°C.

522

523 3.2.4. Effect of the sample concentration

524

525 Fig. 11 shows the separations obtained for [ile]-angiotensin (Fig. 11a) and nadolol (Fig. 11b) by
526 dividing the sample concentration by a factor of 25 and 100, respectively compared to those in Figs.
527 9c and 9d, respectively. Once again, for both solutes, the similarity in the way the separation evolves
528 with the injected volume is absolutely remarkable. It is important to note that all these separations
529 were obtained under linear chromatography conditions. We measured the ratio of the retained peak
530 area to the total area (breakthrough peak and retained peak) for both concentrations and under
531 total breakthrough conditions (1.9% V_0 , red curves in Fig. 11). For both compounds, this ratio was
532 found to be independent of the concentration (about 0.30 for [ile]-angiotensin and 0.25 for nadolol).
533 Similar observations could be drawn for amitriptyline (Fig. S10). Those results are quite consistent
534 with our previous study [7] where we found excellent linearity between the retained peak area and
535 the analyte concentration once total breakthrough conditions were attained.

536

537 4. Conclusions

538 In this work, we have conducted an extensive study on the phenomena of breakthrough and total
539 breakthrough in liquid chromatography. Total breakthrough can be described as a critical case of
540 breakthrough with two distinct peaks for a given solute: an unretained breakthrough peak and a well
541 retained symmetrical peak eluted at the expected retention time. The main objective of this work
542 was to gain some insight into this particular phenomenon and to better define the conditions under

543 which it occurs. To this end, the effect of numerous parameters, including the nature of the solute,
544 the retention mechanism, the injection solvent composition, the injection volume, the gradient
545 elution conditions, the column temperature, and the injected sample concentration, was
546 investigated. Special attention was paid to the impact of these parameters on the emergence of
547 both breakthrough and total breakthrough phenomena. The most important findings from our
548 results are reported below:

- 549 (i) It was previously theoretically established that the injection volume required for
550 breakthrough for a given analyte could be given by a very simple relationship (i.e. $V_{crit,B} = k_S \times$
551 V_0) [16]. In the present experimental study, we have shown that the injection volume
552 required for total breakthrough was found to be about 1.4 times larger in the case of a 30 x
553 2.1-mm column ($V_{crit,TB} = 1.4 \times k_S \times V_0$).
- 554 (ii) Whereas breakthrough might be observed for any compounds as long as the previous
555 relationship is satisfied, the occurrence of total breakthrough seems to be limited to
556 positively charged compounds only. Experimentally, this was confirmed for several weak
557 bases and peptides. Meanwhile, total breakthrough was never reached for negatively
558 charged or neutral compounds whatever the conditions.
- 559 (iii) Considering the importance of the presence of positive charges on the molecule and given
560 that this phenomenon was also observed in HILIC, we believe that the total breakthrough
561 phenomenon could be explained by the circumstances of a mixed retention mechanism.
562 Yet, further investigation should be conducted to confirm this theory and demystify this
563 singular phenomenon. The mechanisms involved must be fully understood before a reliable
564 predictive model can be established as the one proposed for neutral molecules [16]
- 565 (iv) Among all the studied parameters, the injection solvent composition (k_S) and the injection
566 volume (V_i/V_0) for a given analyte were found to be the only ones to have an impact on the
567 onset of breakthrough and total breakthrough. Both phenomena turned out to appear at
568 the same injected volumes regardless of other analytical conditions. This supports the
569 premise that the critical volumes required for breakthrough ($V_{crit,B}$) and total breakthrough
570 ($V_{crit,TB}$) are only dependant on the retention factor of the analyte in the injection solvent (k_S)
571 and the column volume (V_0).
- 572 (v) All the studied parameters seem to act on the retention and shape of the middle peak in
573 contrast to the other peaks (breakthrough and retained peaks).
- 574 (vi) Considering the previously established relationship for $V_{crit,B}$ [16] and based on the above-
575 mentioned conclusions regarding $V_{crit,TB}$, it becomes clear that the only two options to avoid
576 breakthrough, and by extension total breakthrough, for a given analyte, is to reduce the

577 injected volume and/or reduce the eluent strength of the injection solvent. On the other
578 hand, if the goal is to reach total breakthrough, the injection volume should be set so that
579 $V_{crit,TB}$ exceeds $V_{crit,B}$ by a specific factor that was found to be close to 1.4 in the current
580 study. While theoretically, such conditions should be accessible for all compounds as long as
581 they are positively charged, it is worth pointing out that in practice, the required volumes
582 might be very large, hence difficult, if not impossible to reach experimentally in the case of
583 strongly retained compounds injected in weak solvents.

584

585 **References**

586

- 587 [1] D.R. Stoll, P.W. Carr, Two-Dimensional Liquid Chromatography: A State of the Art Tutorial,
588 Anal. Chem. 89 (2017) 519–531. <https://doi.org/10.1021/acs.analchem.6b03506>.
- 589 [2] B.W.J. Pirok, A.F.G. Gargano, P.J. Schoenmakers, Optimizing separations in online
590 comprehensive two-dimensional liquid chromatography, J. Sep. Sci. 41 (2018) 68–98.
591 <https://doi.org/10.1002/jssc.201700863>.
- 592 [3] B.W.J. Pirok, D.R. Stoll, P.J. Schoenmakers, Recent Developments in Two-Dimensional Liquid
593 Chromatography: Fundamental Improvements for Practical Applications, Analytical Chemistry.
594 91 (2019) 240–263. <https://doi.org/10.1021/acs.analchem.8b04841>.
- 595 [4] P. Česla, J. Křenková, Fraction transfer process in on-line comprehensive two-dimensional
596 liquid-phase separations, J. Sep. Sci. 40 (2017) 109–123.
597 <https://doi.org/10.1002/jssc.201600921>.
- 598 [5] Y. Chen, L. Montero, O.J. Schmitz, Advance in on-line two-dimensional liquid chromatography
599 modulation technology, TrAC Trends in Analytical Chemistry. 120 (2019) 115647.
600 <https://doi.org/10.1016/j.trac.2019.115647>.
- 601 [6] G. Vanhoenacker, I. Vandenheede, F. David, P. Sandra, K. Sandra, Comprehensive two-
602 dimensional liquid chromatography of therapeutic monoclonal antibody digests, Anal Bioanal
603 Chem. 407 (2015) 355–366. <https://doi.org/10.1007/s00216-014-8299-1>.
- 604 [7] S. Chapel, F. Rouvière, S. Heinisch, Pushing the limits of resolving power and analysis time in
605 on-line comprehensive hydrophilic interaction x reversed phase liquid chromatography for the
606 analysis of complex peptide samples, Journal of Chromatography A. (2019) 460753.
607 <https://doi.org/10.1016/j.chroma.2019.460753>.
- 608 [8] A. D’Attoma, S. Heinisch, On-line comprehensive two dimensional separations of charged
609 compounds using reversed-phase high performance liquid chromatography and hydrophilic
610 interaction chromatography. Part II: Application to the separation of peptides, Journal of
611 Chromatography A. 1306 (2013) 27–36. <https://doi.org/10.1016/j.chroma.2013.07.048>.
- 612 [9] E. Sommella, O.H. Ismail, F. Pagano, G. Pepe, C. Ostacolo, G. Mazzocanti, M. Russo, E.
613 Novellino, F. Gasparrini, P. Campiglia, Development of an improved online comprehensive
614 hydrophilic interaction chromatography x reversed-phase ultra-high-pressure liquid
615 chromatography platform for complex multiclass polyphenolic sample analysis, J. Sep. Sci. 40
616 (2017) 2188–2197. <https://doi.org/10.1002/jssc.201700134>.
- 617 [10] J.-L. Cao, S.-S. Wang, H. Hu, C.-W. He, J.-B. Wan, H.-X. Su, Y.-T. Wang, P. Li, Online
618 comprehensive two-dimensional hydrophilic interaction chromatography x reversed-phase
619 liquid chromatography coupled with hybrid linear ion trap Orbitrap mass spectrometry for the
620 analysis of phenolic acids in Salvia miltiorrhiza, Journal of Chromatography A. 1536 (2018) 216–
621 227. <https://doi.org/10.1016/j.chroma.2017.09.041>.

- 622 [11] D.R. Stoll, D.C. Harmes, G.O. Staples, O.G. Potter, C.T. Dammann, D. Guillarme, A. Beck,
623 Development of Comprehensive Online Two-Dimensional Liquid Chromatography/Mass
624 Spectrometry Using Hydrophilic Interaction and Reversed-Phase Separations for Rapid and
625 Deep Profiling of Therapeutic Antibodies, *Anal. Chem.* 90 (2018) 5923–5929.
626 <https://doi.org/10.1021/acs.analchem.8b00776>.
- 627 [12] S. Toro-Urbe, L. Montero, L. López-Giraldo, E. Ibáñez, M. Herrero, Characterization of
628 secondary metabolites from green cocoa beans using focusing-modulated comprehensive two-
629 dimensional liquid chromatography coupled to tandem mass spectrometry, *Analytica Chimica*
630 *Acta.* 1036 (2018) 204–213. <https://doi.org/10.1016/j.aca.2018.06.068>.
- 631 [13] Q. Li, F. Lynen, J. Wang, H. Li, G. Xu, P. Sandra, Comprehensive hydrophilic interaction and ion-
632 pair reversed-phase liquid chromatography for analysis of di- to deca-oligonucleotides, *Journal*
633 *of Chromatography A.* 1255 (2012) 237–243. <https://doi.org/10.1016/j.chroma.2011.11.062>.
- 634 [14] P. Jandera, G. Guiochon, Effect of the sample solvent on band profiles in preparative liquid
635 chromatography using non-aqueous reversed-phase high-performance liquid chromatography,
636 *Journal of Chromatography A.* 588 (1991) 1–14. [https://doi.org/10.1016/0021-9673\(91\)85001-](https://doi.org/10.1016/0021-9673(91)85001-V)
637 *V.*
- 638 [15] X. Jiang, A. van der Horst, P.J. Schoenmakers, Breakthrough of polymers in interactive liquid
639 chromatography, *Journal of Chromatography A.* 982 (2002) 55–68.
640 [https://doi.org/10.1016/S0021-9673\(02\)01483-8](https://doi.org/10.1016/S0021-9673(02)01483-8).
- 641 [16] V. Pepermans, S. Chapel, S. Heinisch, G. Desmet, Detailed numerical study of the peak shapes
642 of neutral analytes injected at high solvent strength in short Reversed-Phase liquid
643 chromatography columns and comparison with experimental observations, *Journal of*
644 *Chromatography A.* (2021) 462078. <https://doi.org/10.1016/j.chroma.2021.462078>.
- 645 [17] S. Chapel, F. Rouvière, S. Heinisch, Comparison of existing strategies for keeping symmetrical
646 peaks in on-line Hydrophilic Interaction Liquid Chromatography x Reversed-Phase Liquid
647 Chromatography despite solvent strength mismatch, *Journal of Chromatography A.* 1642
648 (2021) 462001. <https://doi.org/10.1016/j.chroma.2021.462001>.
- 649 [18] D.V. McCalley, Effect of temperature and flow-rate on analysis of basic compounds in high-
650 performance liquid chromatography using a reversed-phase column, *Journal of*
651 *Chromatography A.* 902 (2000) 311–321. [https://doi.org/10.1016/S0021-9673\(00\)00924-9](https://doi.org/10.1016/S0021-9673(00)00924-9).
- 652 [19] B. Buszewski, S. Noga, Hydrophilic interaction liquid chromatography (HILIC)—a powerful
653 separation technique, *Anal Bioanal Chem.* 402 (2012) 231–247.
654 <https://doi.org/10.1007/s00216-011-5308-5>.
- 655 [20] D.V. McCalley, Understanding and manipulating the separation in hydrophilic interaction liquid
656 chromatography, *Journal of Chromatography A.* 1523 (2017) 49–71.
657 <https://doi.org/10.1016/j.chroma.2017.06.026>.
- 658
- 659

660 Figure captions:

661

662 Fig. 1: Occurrence of breakthrough and total breakthrough in gradient elution at acidic pH for (a)
663 caffeine (2 mg/L), (b) leucine enkephalin (50 mg/L), (c) propranolol (0.5 mg/L), and (d) salicylic acid
664 (25 mg/L). Injection solvent: 50% ACN. Increased injection volumes (V_i/V_0) from top to bottom.
665 Acquity CSH C18 column (30 x 2.1 mm, 1.7 μ m); 1.5 mL/min; 80°C; Mobile phase : A: water + 0.1%
666 FA, B: ACN + 0.1% FA; 1-45-1-1% B in 0-0.54-0.59-1 min (normalized gradient slope of 4%). The
667 gradient profile at the column outlet is given in dotted line with the composition scale on the right.
668 The asterisk indicates the non-retained breakthrough peak. ESI-MS detection.

669

670 Fig.2: Occurrence of breakthrough and total breakthrough in isocratic elution at acidic pH for leucine
671 enkephalin (0.5 mg/L). Injection solvent: 50% ACN. Increased injection volumes (V_i/V_0) from top to
672 bottom. 0.5 mL/min; mobile phase A: water + 0.1% FA, B: ACN + 0.1% FA (90:10 A/B). Same other
673 conditions as in Fig. 1. The asterisk indicates the non-retained breakthrough peak.

674

675 Fig.3: Occurrence of Breakthrough and total breakthrough in gradient elution at neutral pH for (a)
676 leucine enkephalin (5 mg/L), (b) NN-dimethylaniline (0.05 mg/L), and (d) salicylic acid (25 mg/L).
677 Injection solvent: 70% ACN (a, b) or 50% ACN (c). Increased injection volumes (V_i/V_0) from top to
678 bottom. Acquity CSH C18 column (30 x 2.1 mm, 1.7 μ m); 0.75 mL/min; 30°C; mobile phase : A: water
679 + ammonium acetate 10 mM, B: ACN; 1-55-1-1% B in 0-1.33-1.43-3 min (normalized gradient slope
680 of 4%). The gradient profile at the column outlet is given in dotted line with the composition scale on
681 the right. The asterisk indicates the non-retained breakthrough peak. ESI-MS detection.

682

683 Fig.4: Occurrence of breakthrough and total breakthrough in HILIC for leucine enkephalin (32 mg/L).
684 Injection solvent: 100% water. Increased injection volumes (V_i/V_0) from top to bottom. Acquity BEH
685 Amide column (50 x 2.1 mm, 1.7 μ m); 0.6 mL/min; 30°C; mobile phase : A: ACN and B: water +
686 ammonium acetate 10 mM (pH 6.8); 2-60-2-2% B in 0-5.8-6-8 min (normalized gradient slope of 2%).
687 UV detection at 210 nm. The gradient profile at the column outlet is given in dotted line with the
688 composition scale on the right. The asterisk indicates the non-retained breakthrough peak.

689

690 Fig.5: Effect of the injection solvent composition on the separation: (a) 30% ACN, (b) 50% ACN, (c)
691 70% ACN, and (d) 90% ACN. V_i/V_0 was varied from 1% to 50% ACN. Solute: leucine enkephalin (50
692 mg/L). Same other conditions as in Fig. 1.

693

694 Fig.6: Effect of the initial composition (C_{initial}) on the separation: (a) 1% ACN, (b) 5% ACN, and (c) 10%
695 ACN. The normalized gradient slope was maintained at 4% by changing the gradient time : (a) 0.54
696 min, (b) 0.49 min, (c) 0.43 min. Injection volume (V_i/V_0) = 2.5%. Solute: leucine enkephalin (50 mg/L).
697 Same other conditions as in Fig. 1. The asterisk indicates the non-retained breakthrough peak.

698

699 Fig.7: Effect of the gradient time on the separation. The gradient time is expressed as a multiple of
700 the column dead time (t_0): (a) $44t_0$, (b) $11t_0$, (c) $5.5t_0$, and (d) $3.7t_0$, ($t_0 = 0.049\text{min}$). The resulting
701 normalized gradient slope is given in brackets. V_i/V_0 was varied from 1% to 6.9%. Solute: leucine
702 enkephalin (50 mg/L). Same other conditions as in Fig. 1.

703

704 Fig.8: Effect of the initial isocratic hold duration on the separation: (a) 0 min, (b) 0.13 min, and (c)
705 0.53 min. Gradient time : 1.08 min (normalized gradient slope of 4%). V_i/V_0 was varied from 1% to
706 1.5%. Solutes: [ile]-angiotensin (100 mg/L) and (D-F) nadolol (0.5 mg/L). Flow rate: 0.75 mL/min.
707 Same other conditions as in Fig. 1.

708

709 Fig.9: Effect of the flow rate on the separation: (a, b): 1.5 mL/min with a gradient time of 0.54 min
710 and (c, d) 0.75 mL/min with a gradient time of 1.08 min. 80°C; Solute: (a, c) [ile]-angiotensin (250
711 mg/L) and (b, d) nadolol (0.5 mg/L). V_i/V_0 was varied from 1% to 1.9%. Same other conditions as in
712 Fig. 1.

713

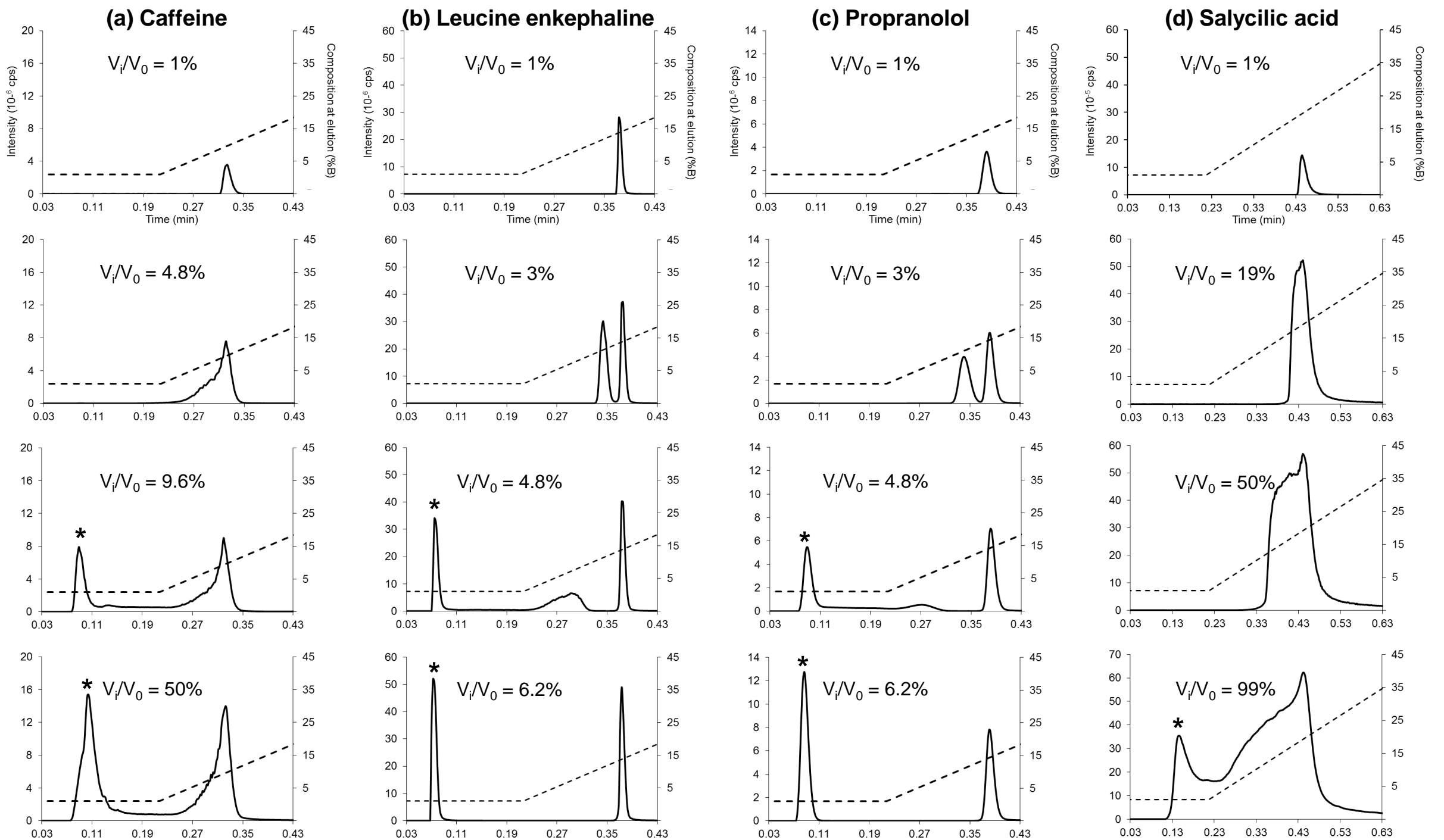
714 Fig.10: Effect of a decrease in column temperature (30°C) on the separation of (a) [ile]-angiotensin
715 (250 mg/L) and (b) nadolol (0.5 mg/L). Same other conditions as in Figs. 9c and 9d.

716

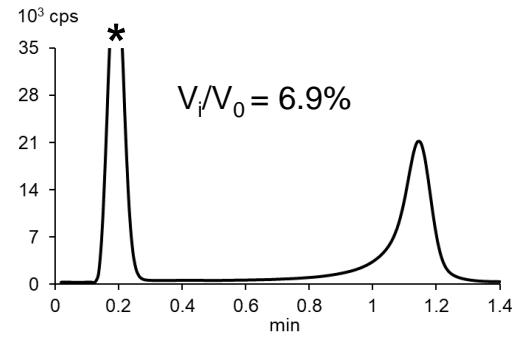
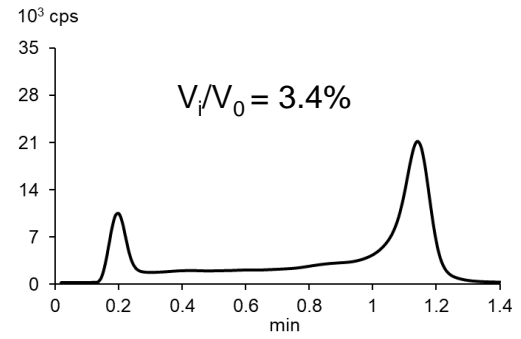
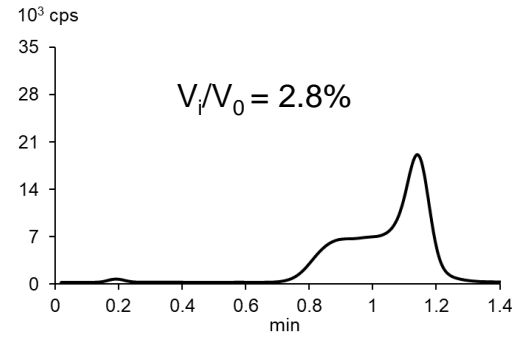
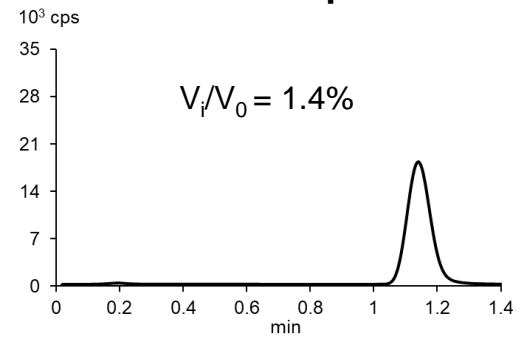
717 Fig.11: Effect of a decrease in sample concentration on the separation of (a) [ile]-angiotensin (10
718 mg/L) and (b) nadolol (0.005 mg/L). Same other conditions as in Figs. 9c and 9d.

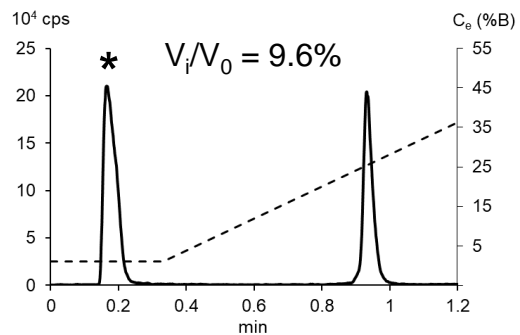
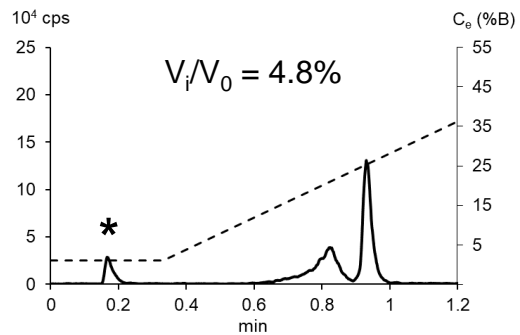
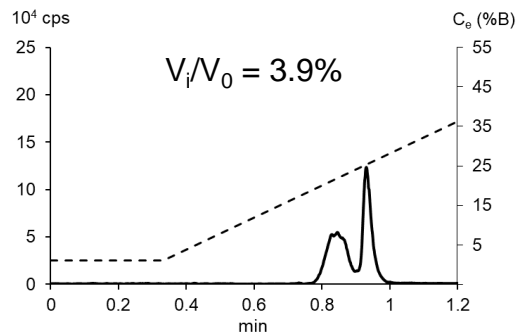
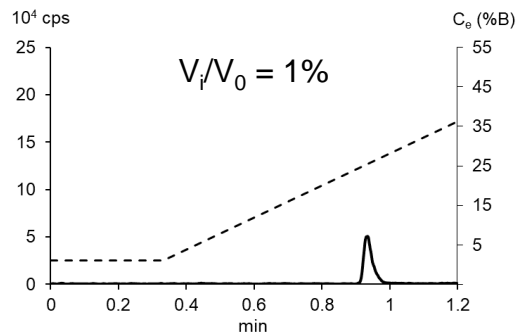
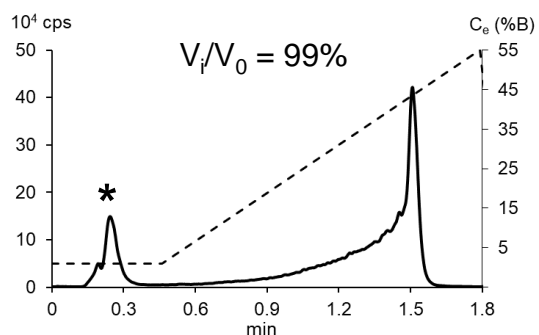
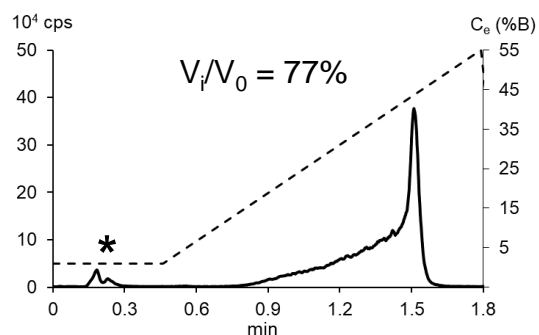
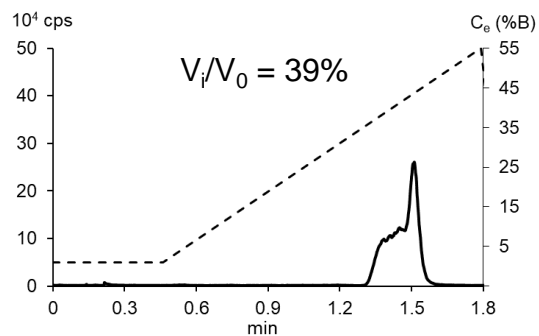
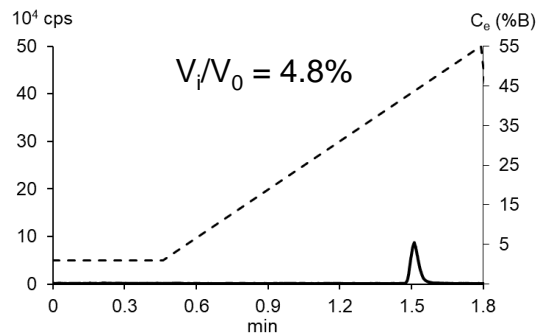
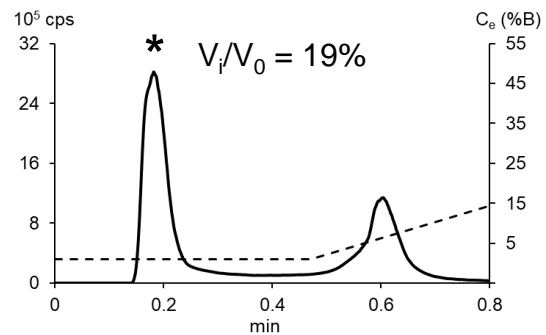
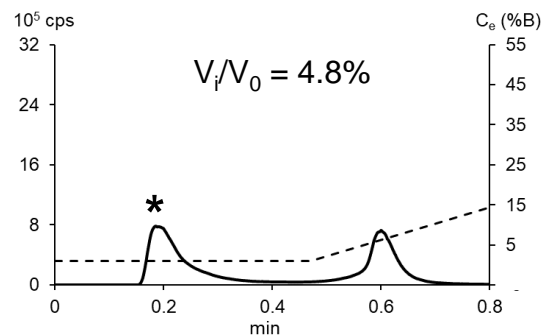
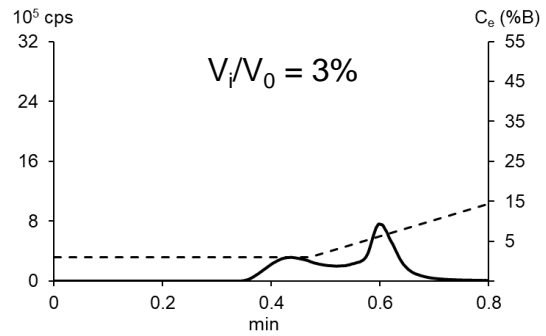
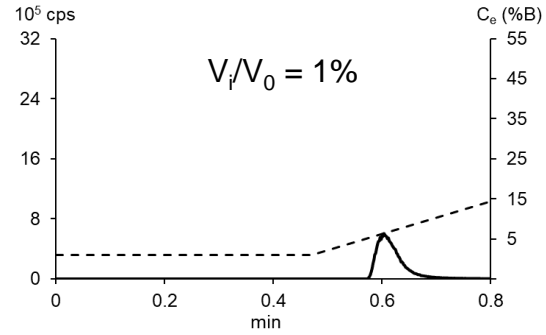
719

720

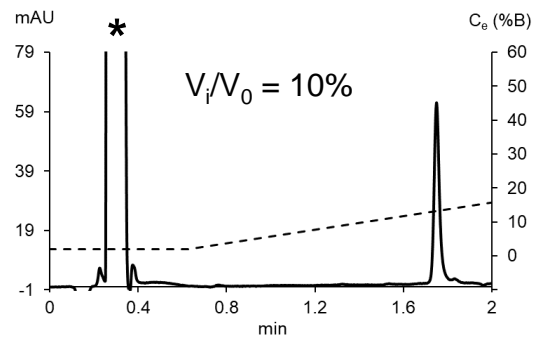
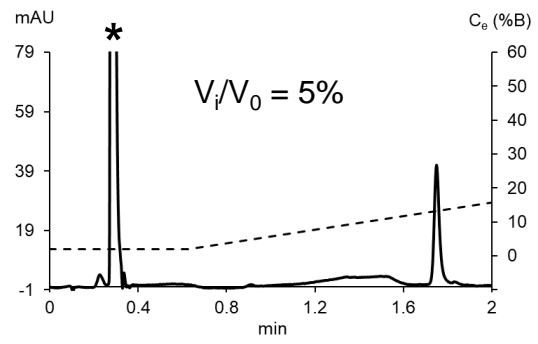
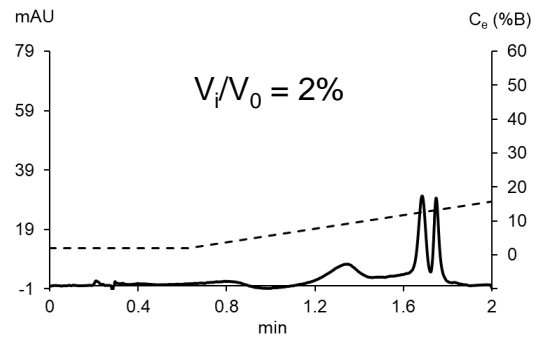
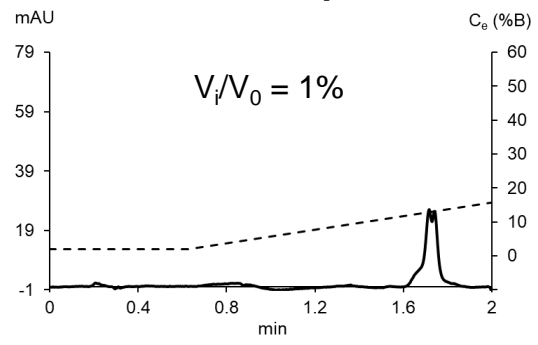


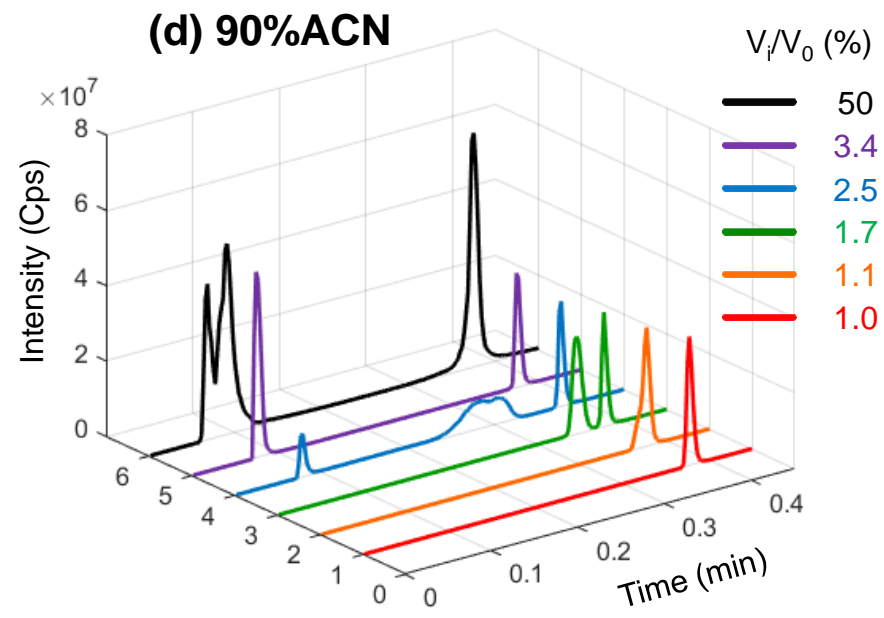
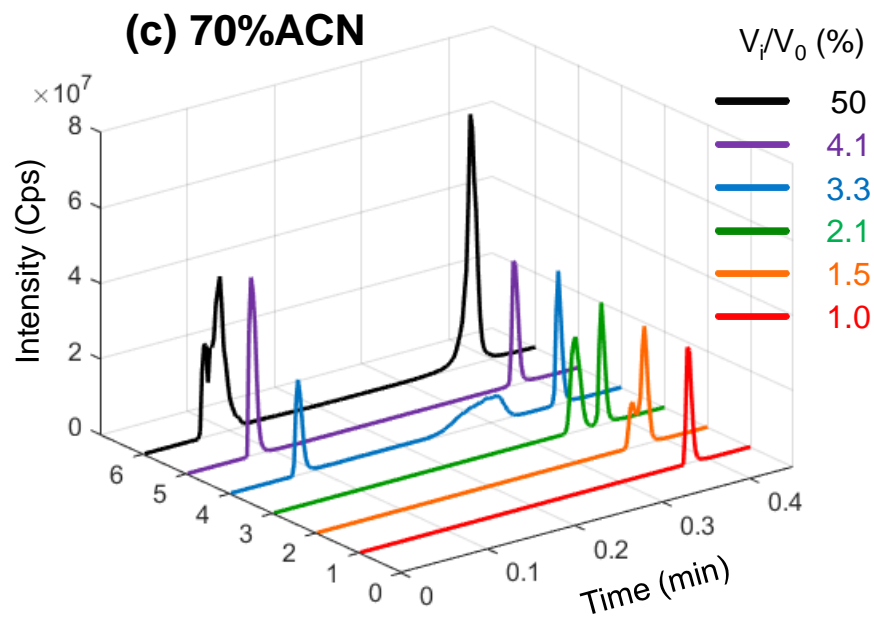
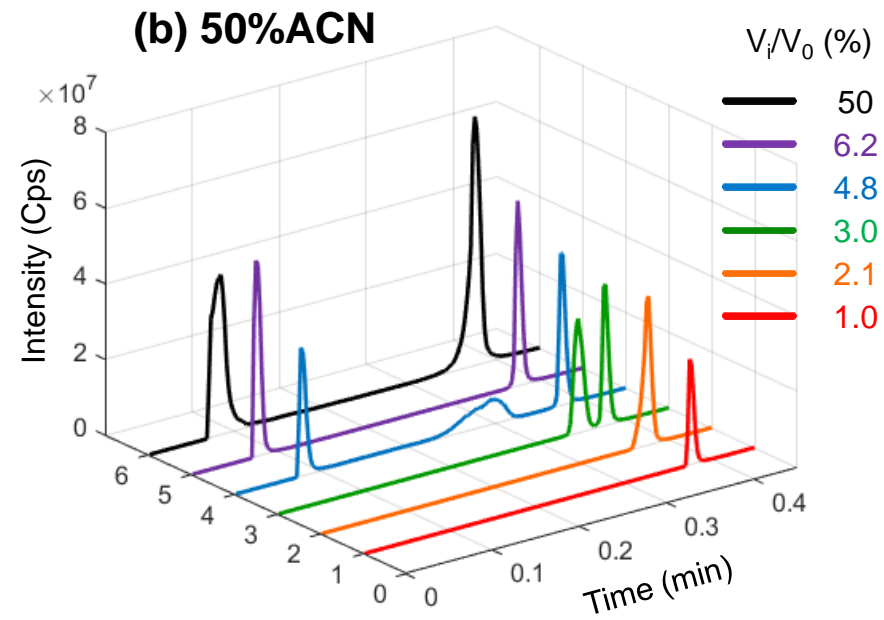
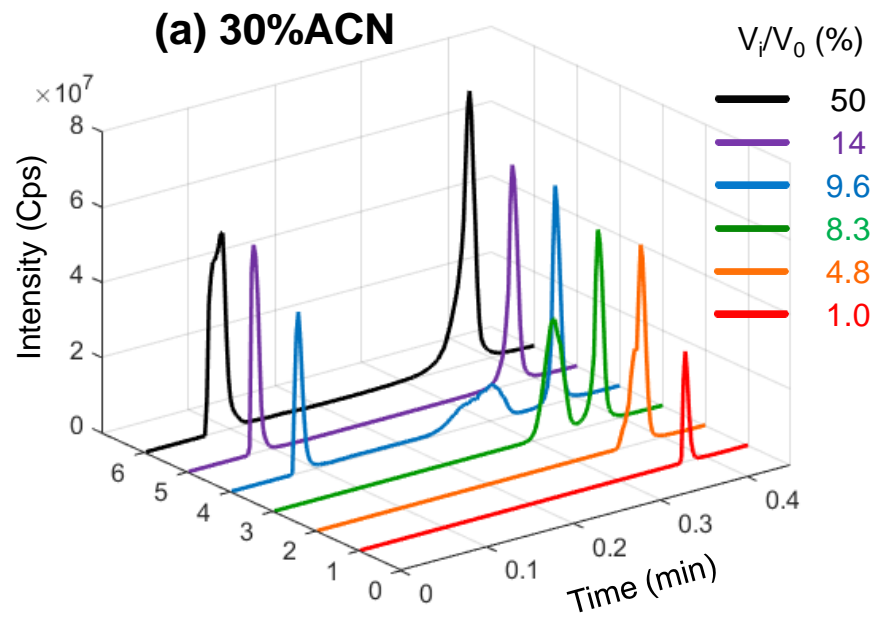
Leucine enkephalin

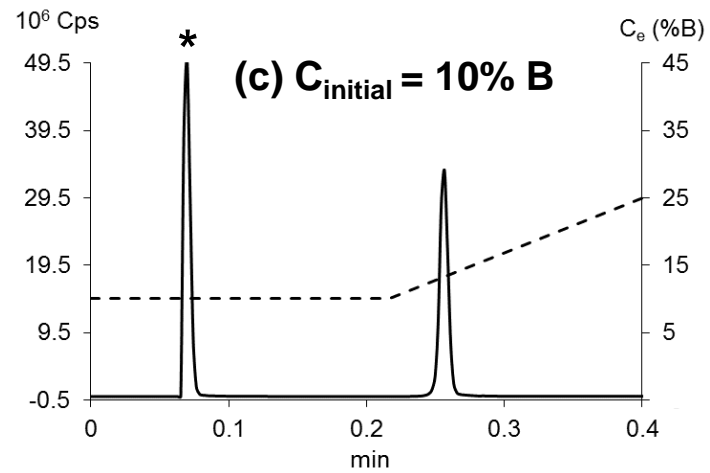
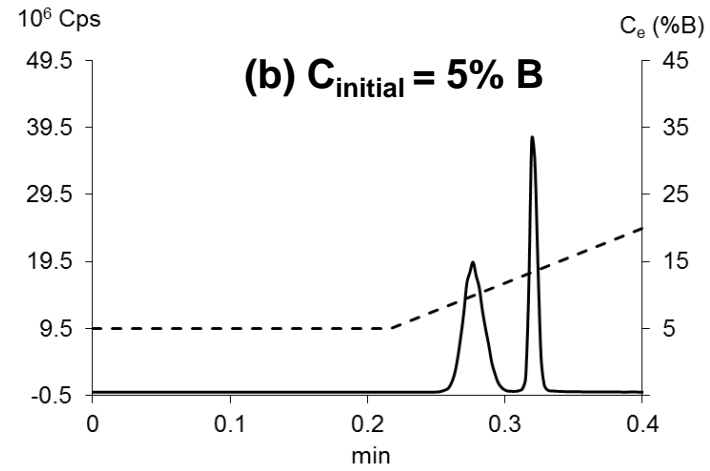
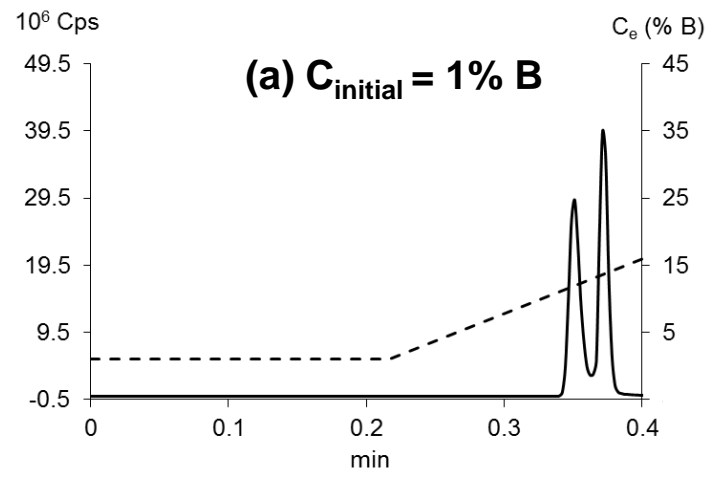


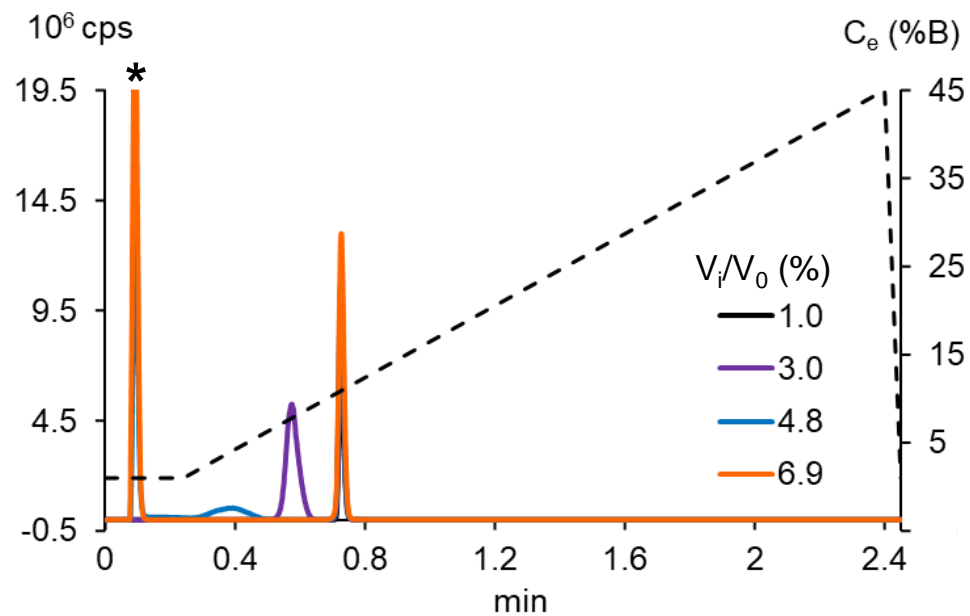
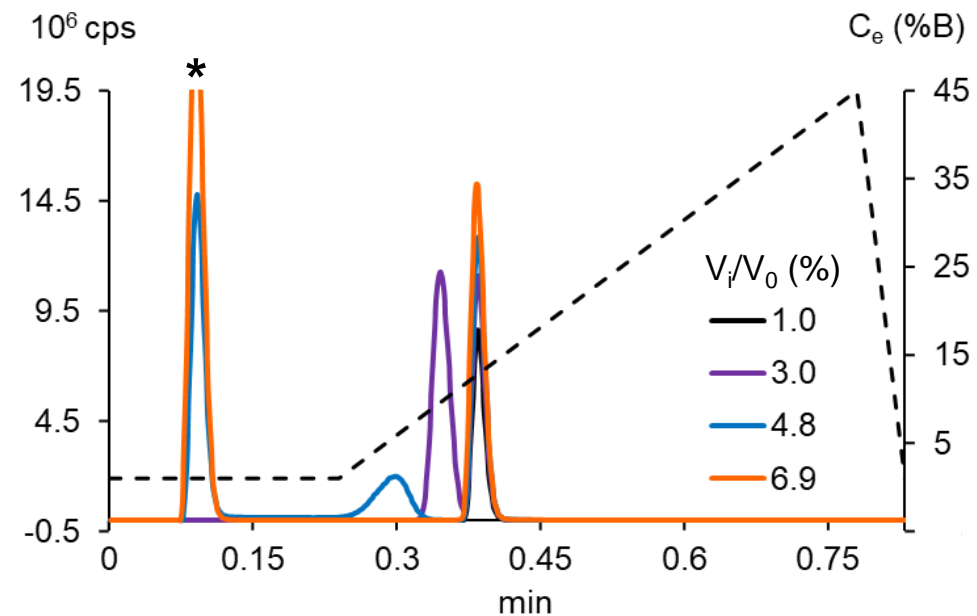
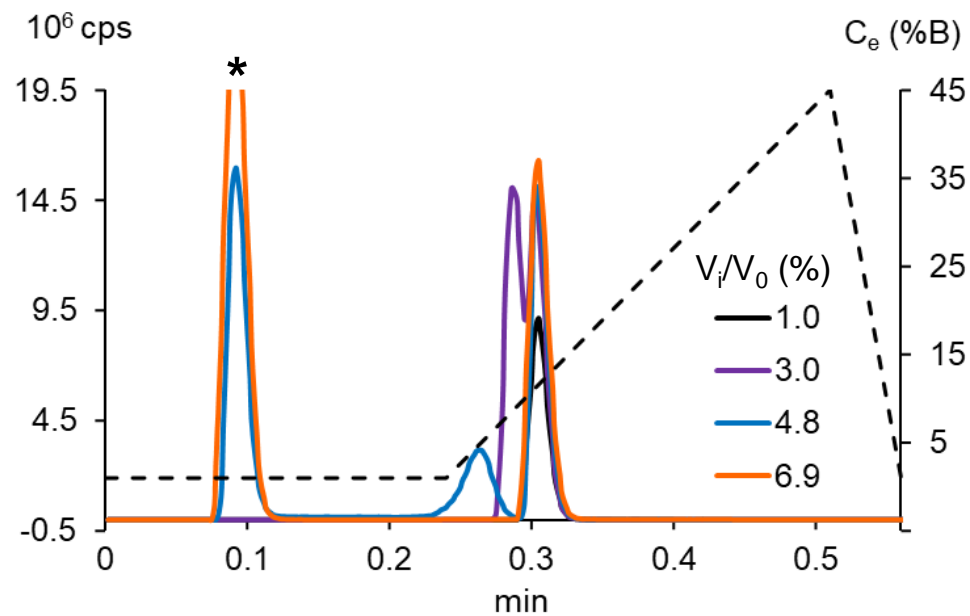
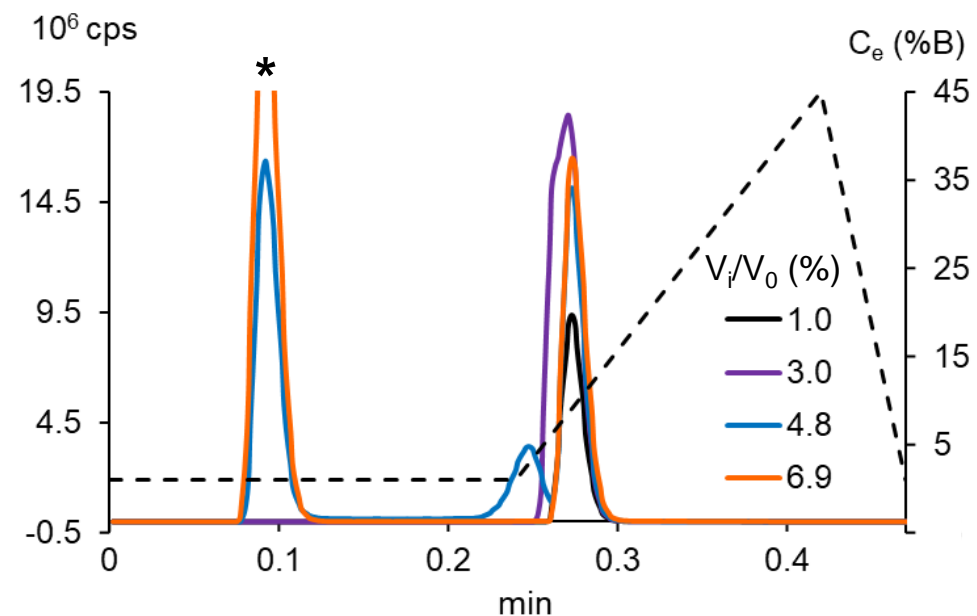
(a) Leucine enkephaline**(b) NN-dimethylaniline****(c) Salycilic acid**

Leucine enkephaline

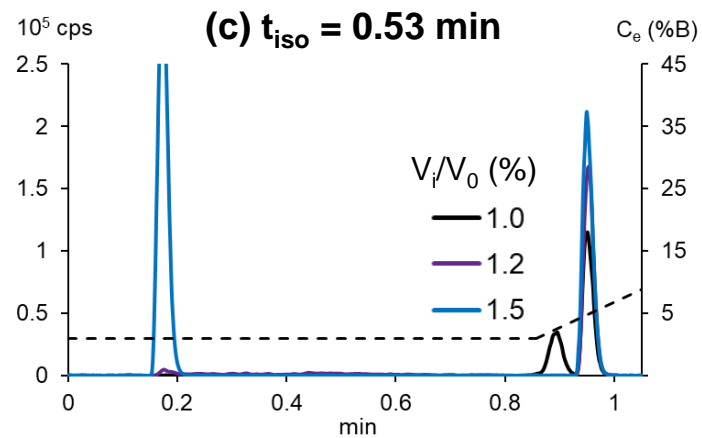
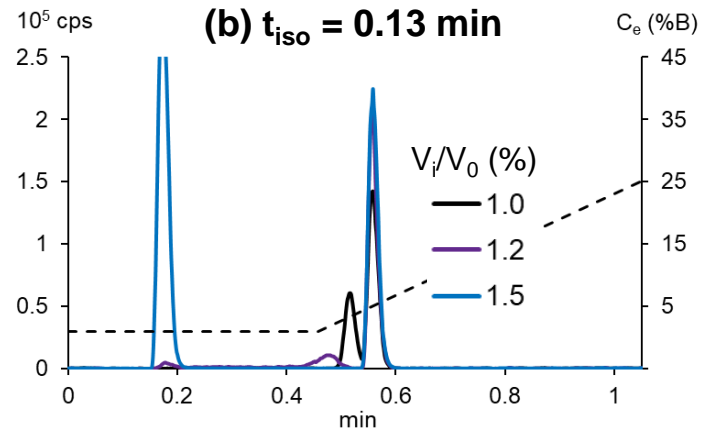
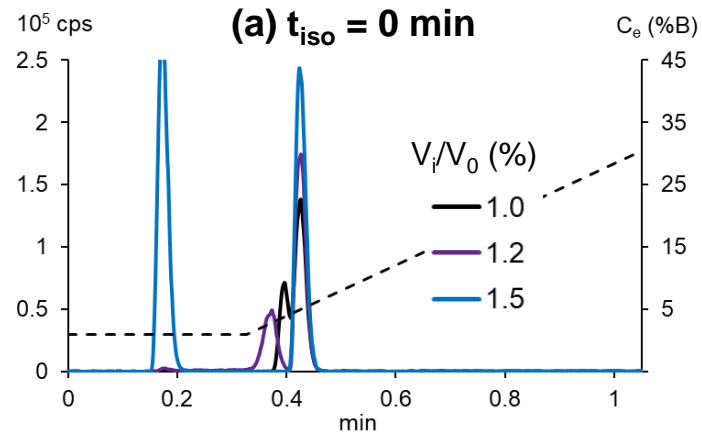




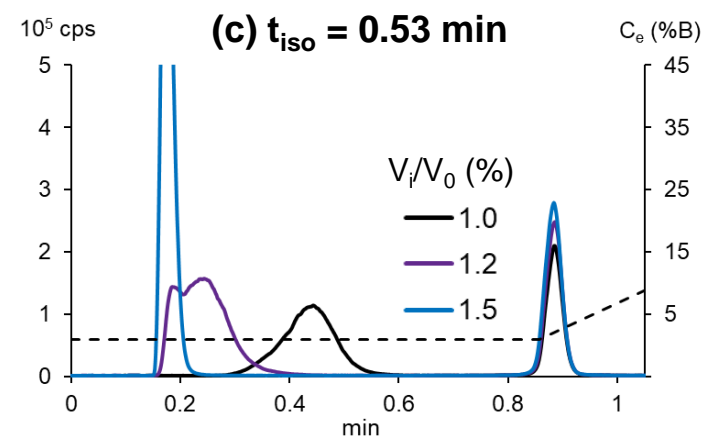
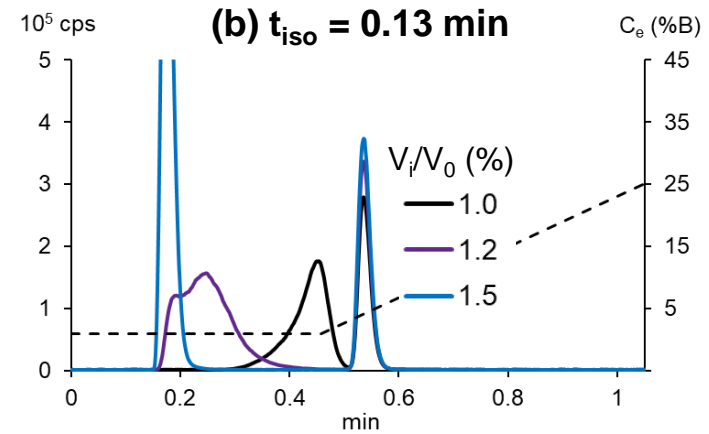
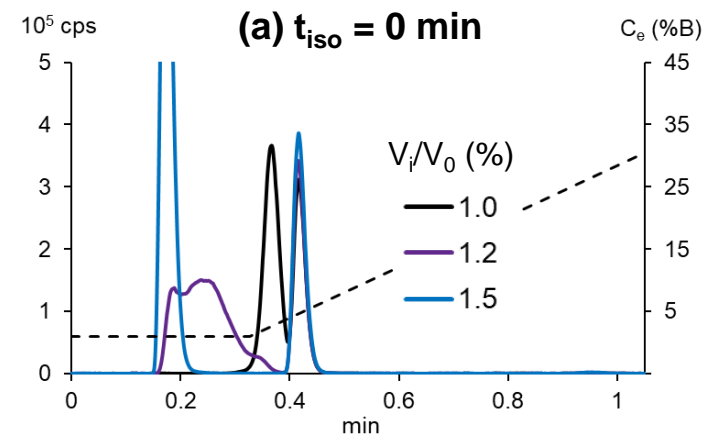


(a) $t_G = 44 t_0$ (1%)**(b) $t_G = 11 t_0$ (4%)****(c) $t_G = 5.5 t_0$ (8%)****(d) $t_G = 3.7 t_0$ (12%)**

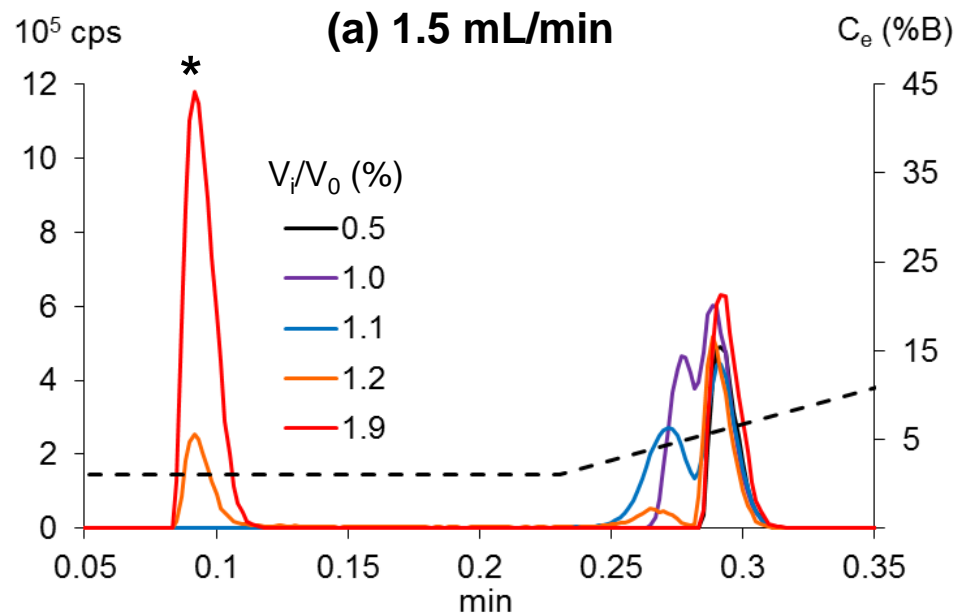
[ile]-angiotensin



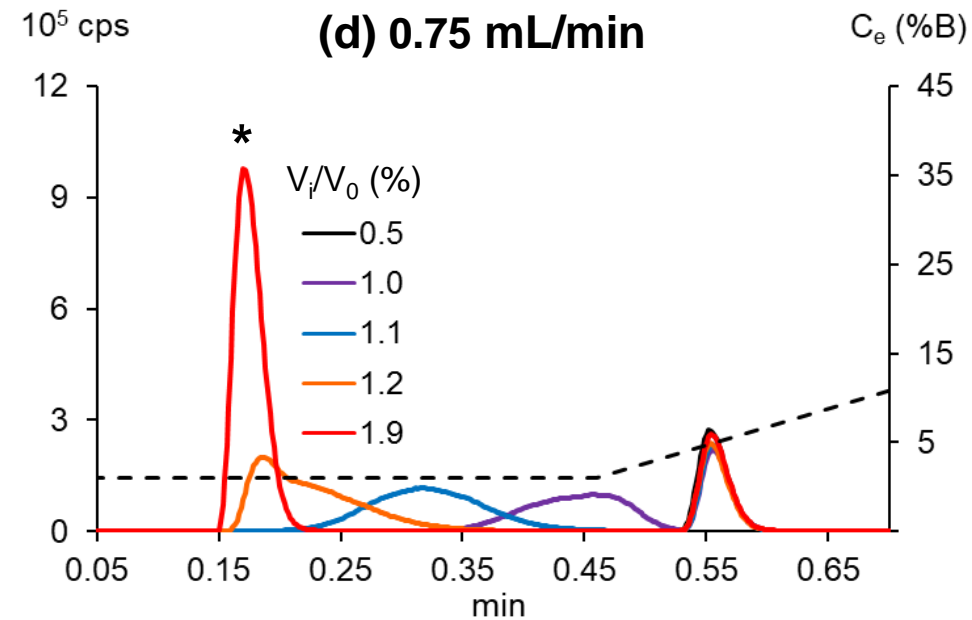
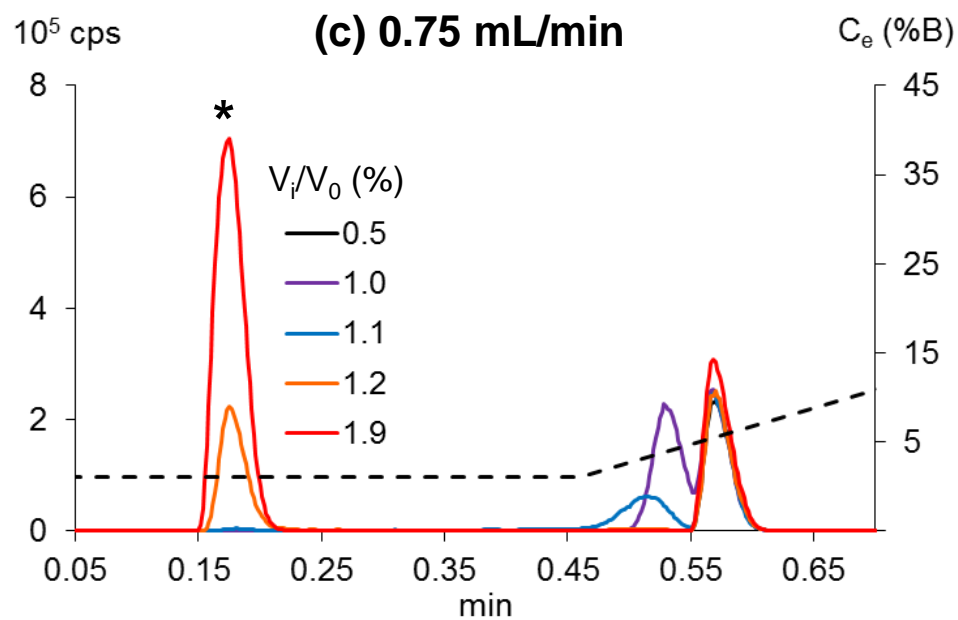
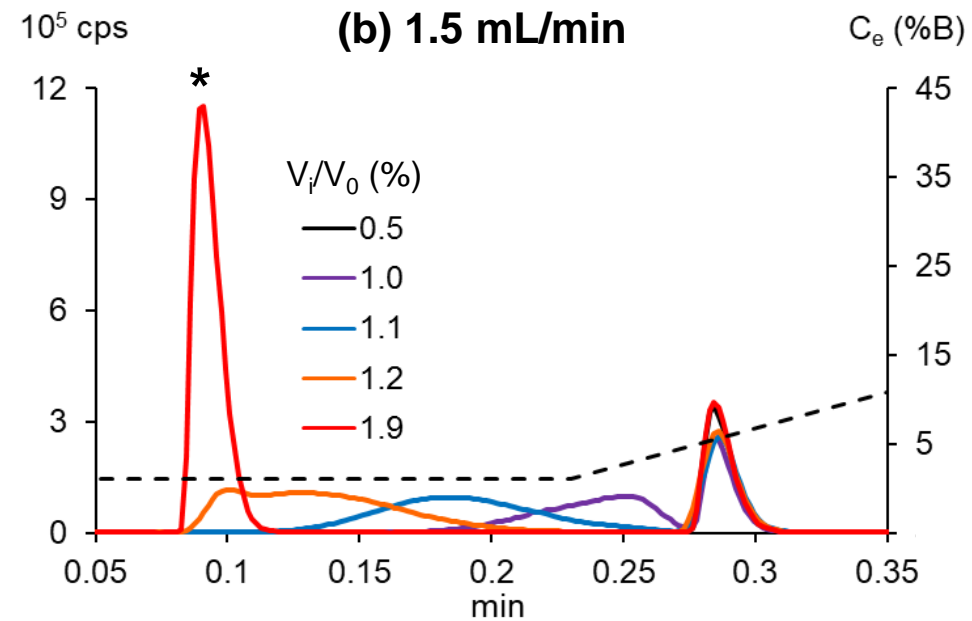
Nadolol



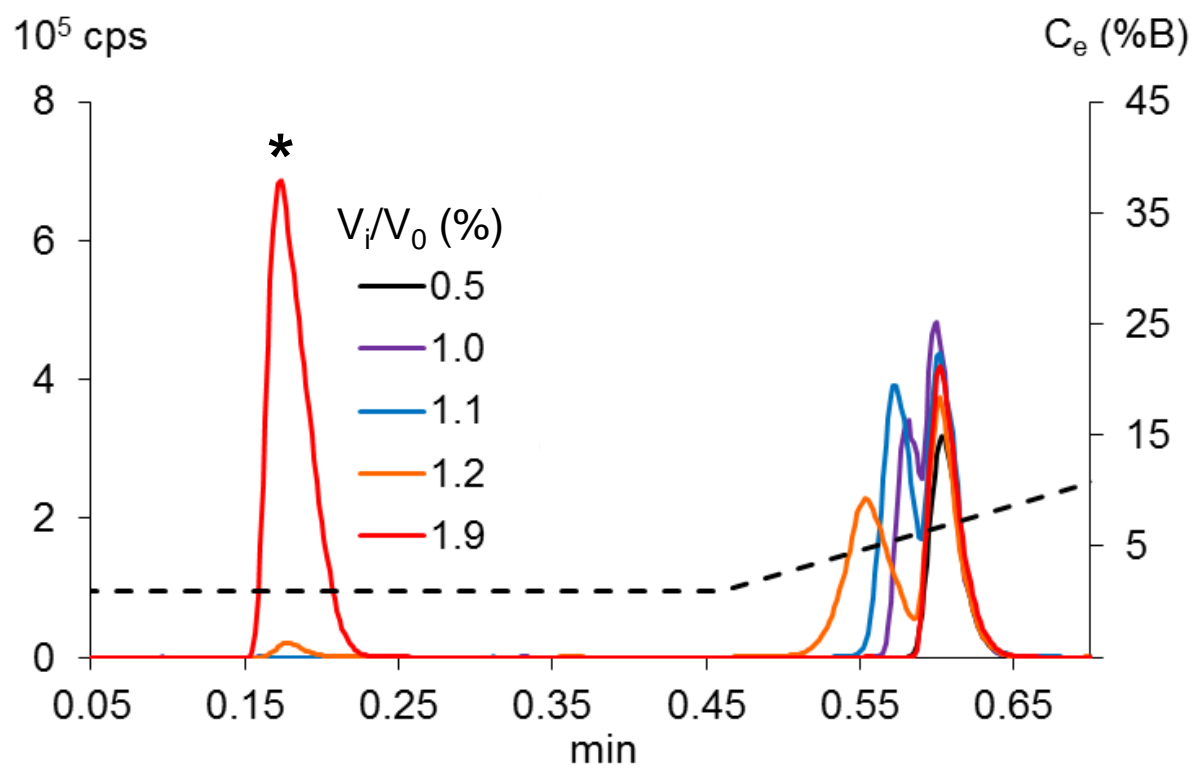
[ile]-angiotensin



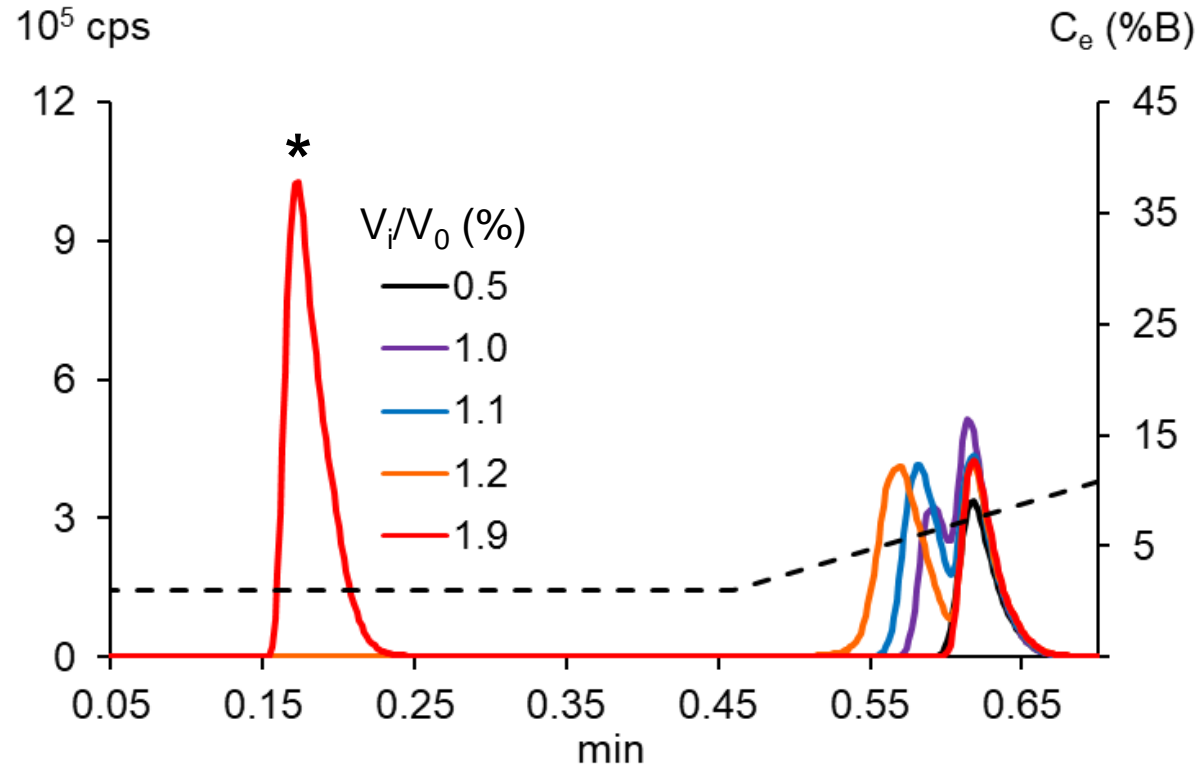
Nadolol



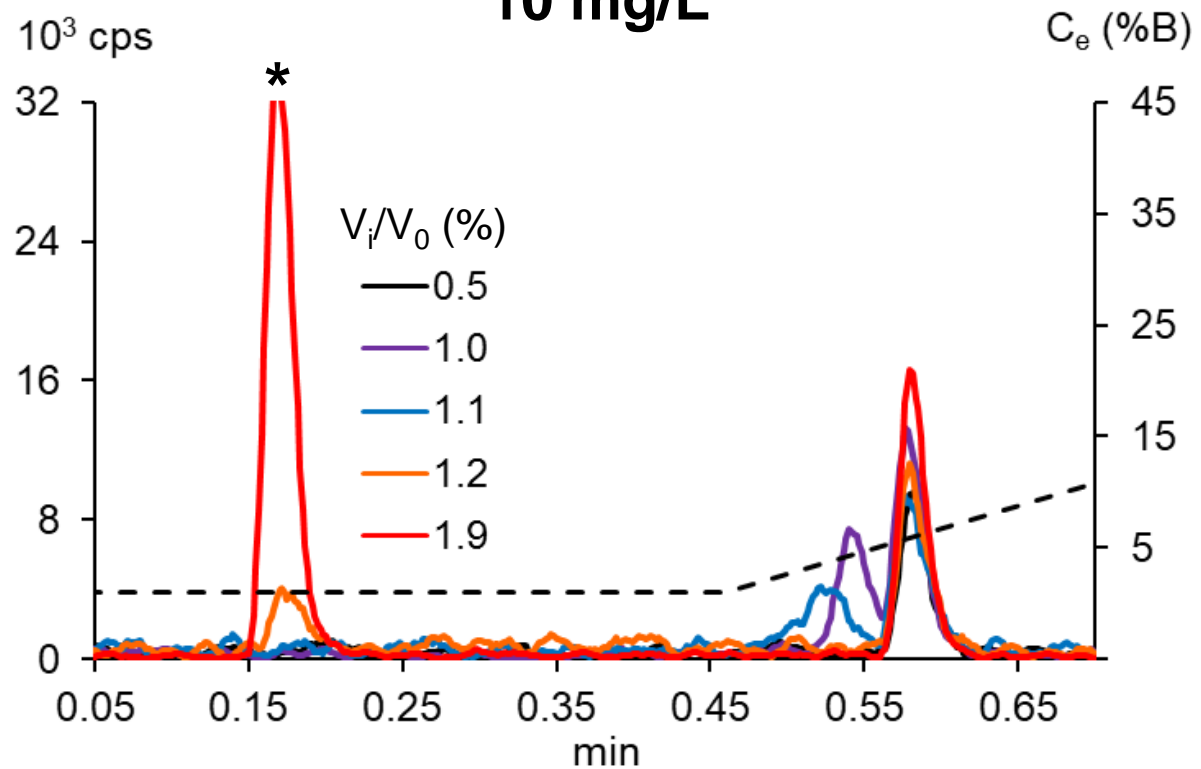
(a) [ile]-angiotensin



(b) Nadolol



**(a) [ile]-angiotensin
10 mg/L**



**(b) Nadolol
0.005 mg/L**

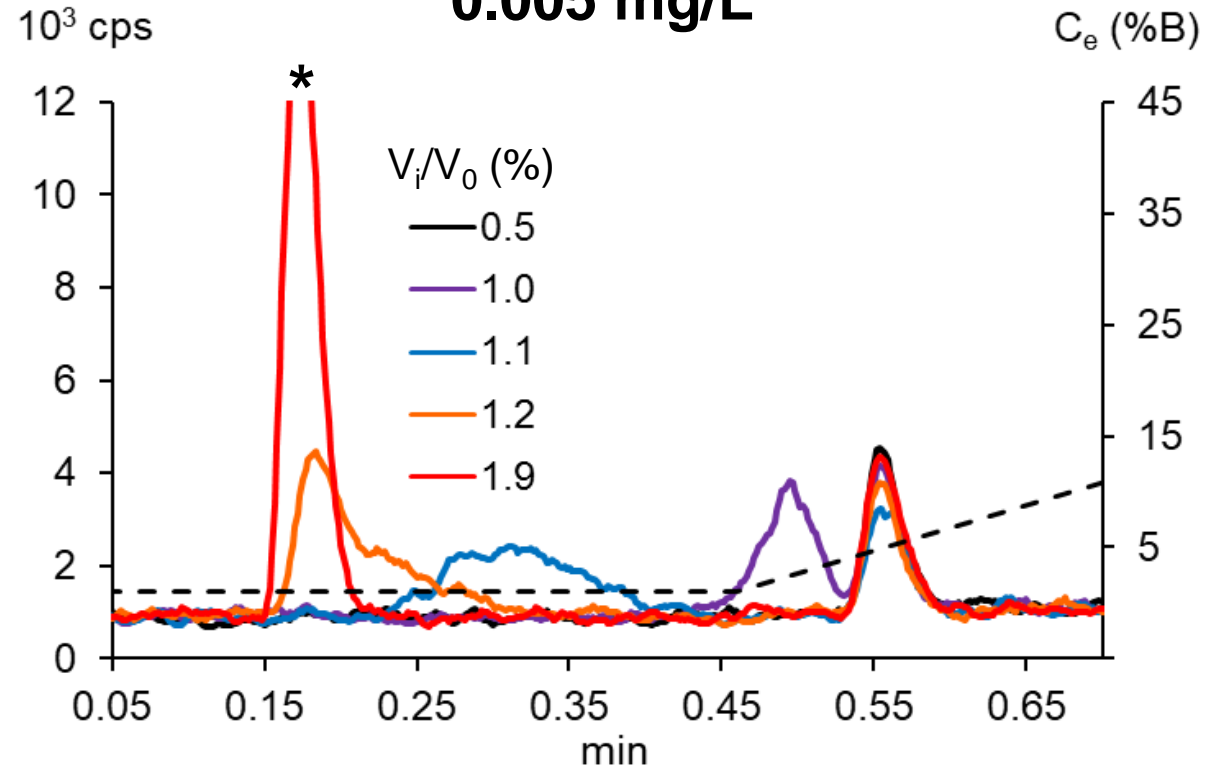


Table 1: Characteristics and Physical properties of the studied compounds.

| # | Compound | m/z (Da) | Pi or pKa (25°C) | S _{log} | Log(k _w) |
|----|------------------------------|----------|------------------|------------------|----------------------|
| P1 | Influenza hemagglutinin (HA) | 1103.2 | 3.5 | 16.5 | 3.04 |
| P2 | Leucine enkephalin | 556.6 | 6.0 | 11.4 | 2.22 |
| P3 | [arg8]-Vasopressin | 543.1* | 8.2 | 21.1 | 1.52 |
| P4 | [ile]-Angiotensin | 898.1 | 9.4 | 20.9 | 1.94 |
| P5 | Bradykinin fragment 1-5 | 573.7 | 10.6 | 15.6 | 1.07 |
| P6 | Substance P | 674.8* | 11.7 | 20.6 | 3.25 |
| P7 | Bradykinin | 531.1* | 12.5 | 20.5 | 2.22 |
| B1 | N,N-dimethylaniline | 122.2 | 5.1 | 10.5 | 2.29 |
| B2 | diphenhydramine | 256.4 | 8.8 | 9.7 | 2.10 |
| B3 | propranolol | 260.3 | 9.1 | 10.7 | 2.03 |
| B4 | amitriptyline | 278.4 | 9.2 | 9.3 | 2.64 |
| B5 | nadolol | 310.4 | 9.2 | 23.6 | 1.64 |
| N1 | Caffeine | 193.2 | 1.4 | | |
| A1 | Salicylic acid | 137.1 | 3.0 | | |

*dicharged ion